# Serotonin and common antidepressants regulate lipoprotein(a) macropinocytosis via enhanced cell surface binding.

Gregory MI Redpath[1,2]*, Nikita Deo[1,2]*, Halima Siddiqui[1,2], Golnoush Madani[1.2], Natasha Kapoor-Kaushik[3], Nicholas Ariotti[3], Malcolm Rutledge[1,2], Michael JA Williams[2,4], Sally PA McCormick[1,2].

***Affiliations***:
[1] Department of Biochemistry, University of Otago, Dunedin, New Zealand.
[2] HeartOtago, University of Otago, Dunedin, New Zealand.
[3] Electron Microscopy Unit, Mark Wainwright Analytical Centre, University of New South Wales, NSW, Sydney, Australia.
[4] Department of Medicine, Dunedin School of Medicine, University of Otago, Dunedin, New Zealand.

*These authors contributed equally to this work.

***Corresponding author***:
Professor Sally PA McCormick
Correspondence: sally.mccormick@otago.ac.nz

## Summary

Elevated lipoprotein(a) (Lp(a)) levels have been found in individuals suffering from depression posing an increased risk of cardiovascular disease (CVD). Efforts to effectively reduce circulating Lp(a) levels have been limited due to an inability to ascribe a clear cellular uptake pathway, despite multiple receptors being implicated in Lp(a) uptake. We report here that Lp(a) uptake is mediated by the fluid-phase endocytic process, macropinocytosis. Furthermore, serotonin and commonly prescribed antidepressants promote Lp(a) uptake by macropinocytosis in liver cells by increasing cell surface association. These findings represent a major paradigm shift in Lp(a) biology since previous studies have attributed Lp(a) uptake to receptor-mediated endocytosis. They also imply that treatment with antidepressants may improve cardiovascular as well as mental health.

## Abstract.

Multiple receptors have been implicated in lipoprotein(a) (Lp(a)) uptake, yet each receptor only partially accounts for the uptake, and no endocytic pathway has been described for Lp(a) internalisation to date. In this study, we define macropinocytosis as the endocytic pathway responsible for internalising Lp(a). In liver and macrophage cells, Lp(a) uptake was dependent on extracellular calcium and inhibited by amiloride or its derivative EIPA (5-(N-ethyl-N-isopropyl)-Amiloride). Uptake of the unique protein component of Lp(a), apolipoprotein(a) (apo(a)) alone was also dependent on macropinocytosis, indicating that it is the likely mediator of Lp(a) uptake. In macrophages, the tricyclic antidepressant, imipramine, and the selective serotonin reuptake inhibitors (SSRIs) citalopram, fluoxetine and sertraline all inhibited Lp(a) uptake, likely due to macrophage de-differentiation effects and dynamin inhibition (in the case of sertraline). In liver cells, imipramine and citalopram strongly stimulated Lp(a) uptake, while sertraline inhibited uptake. Imipramine and citalopram enhanced cell surface binding of Lp(a) rather than upregulating macropinocytosis *per se*, indicating that immobilisation on the plasma membrane is an important step in Lp(a) macropinocytosis. Serotonin treatment also increased Lp(a) cell surface binding, promoting subsequent macropinocytotic uptake, consistent with imipramine and citalopram boosting extracellular serotonin levels through serotonin transporter inhibition. Imipramine and citalopram increased Lp(a) delivery to Rab11-positive recycling endosomes which promoted recycling of the apo(a) component of Lp(a) into the culture media. These findings support the utility of imipramine and citalopram as promising Lp(a)-lowering therapeutics in people suffering from depression who often have elevated Lp(a) levels and an increased risk of cardiovascular disease.

**Keywords*:* lipoprotein(a) | macropinocytosis | endosomal sorting | atherosclerosis | selective serotonin reuptake inhibitors | Rab11 | depression | endocytosis | serotonin**

## Introduction

Lipoprotein(a) (Lp(a)) is a highly atherogenic form of low-density lipoprotein (LDL)[1]. Lp(a) consists of an LDL-like particle containing apolipoprotein-B (apoB), covalently bound to apolipoprotein(a) (apo(a)), a glycoprotein that is structurally similar to plasminogen[2].

Lp(a) is elevated (greater than 100 nmol) in at least 20% of the population[3] and recent data from the United Kingdom Biobank indicates that every 50 nmol increment increase in Lp(a) imparts a greater risk of cardiovascular disease (CVD) development[4]. While LDL is often referred to as the "bad" cholesterol, elevated Lp(a) levels are frequently overlooked despite having an equal impact on CVD development and risk[5]. Unlike with LDL, specific Lp(a) lowering treatments remain limited, with RNA antisense therapy targeted to apo(a) being the only treatment close to becoming clinically available[6]. Understanding how LDL is cleared from circulation by endocytosis has led to the development of statins and newer therapies such as PCSK9 inhibitors[7] to lower LDL. Despite the importance of endocytic processes in lipoprotein clearance, little is known about the endocytic regulation of Lp(a). The inability to ascribe a clear single receptor that mediates Lp(a) uptake has hampered the development of effective therapies for Lp(a) lowering.

Multiple receptors have been implicated in binding Lp(a) and mediating Lp(a) endocytic uptake into the cell including the LDL receptor[8–11] , VLDL receptor[12] and plasminogen receptors[13], yet in each case the impact of each receptor on Lp(a) uptake is either inconsistent or only partially responsible for uptake, leaving our understanding of the process of Lp(a) catabolism incomplete[11,14–17]. Given the multitude of receptors implicated in Lp(a) uptake without any clearly defined mechanistic role in Lp(a) endocytosis, we hypothesised that Lp(a) uptake occurs *via* the endocytic process called macropinocytosis.

There are many pathways of endocytosis identified to date, each with specific cargoes, activation conditions and functions[18]. Clathrin-dependent and fast endophilin mediated endocytosis represent mechanisms of receptor-mediated endocytosis. In both cases, cargo/ligand binding to the receptor leads to the assembly of adaptor and coat proteins around the forming endosome which promote receptor and cargo internalisation[19–22]. In contrast, macropinocytosis is a calcium-dependent endocytic pathway where cargo is internalised *via* membrane remodelling events as opposed to receptor-mediated initiation of endocytosis. Macropinocytosis requires extracellular calcium to initiate an intracellular signalling cascade which stimulates characteristic actin remodelling required for engulfment of cargoes[23]. To date a requirement for extracellular calcium has not been documented for other forms of endocytosis in non-neuronal cell types[22,24–26]. Macropinocytosis is not defined by specific protein or cellular markers, although large dextran polymers (70 kDa and above) have been shown to be *bona fide* macropinocytosis cargo and thus often used as a marker of the process[27].

We determined that macropinocytosis was a key endocytic pathway regulating Lp(a) uptake in liver cells, likely through the apo(a) protein component. Consistent with this, we found EGTA effectively inhibited Lp(a) uptake in liver cells and THP-1 macrophages. Amiloride and its derivative EIPA effectively inhibits macropinocytosis by preventing activation of the GTPases, Rac1 and CDC42, which are required for actin remodelling[28]. Accordingly, we found that these inhibitors significantly diminished Lp(a) uptake in liver cells and macrophages, identifying macropinocytosis as a key endocytic mechanism in Lp(a) uptake. Using the tricyclic antidepressant imipramine, a recently identified macropinocytosis inhibitor[29], we found Lp(a) uptake was partially inhibited in macrophages. Surprisingly, imipramine *stimulated* Lp(a) uptake in liver cells, leading us to determine the effects of commonly used selective serotonin reuptake inhibitor (SSRI) antidepressants on Lp(a) uptake. Citalopram also robustly stimulated Lp(a) uptake in liver cells while sertraline inhibited Lp(a) uptake, likely due to its effects as a dynamin inhibitor.

Finally, we defined how imipramine and citalopram regulated Lp(a) uptake. Neither drug directly affected macropinocytosis, but stimulated Lp(a) binding to the cell surface. Serotonin treatment also enhanced Lp(a) cell surface binding and subsequent uptake by macropinocytosis. Imipramine and citalopram therefore likely exert their effects by enhancing extracellular serotonin levels through serotonin transporter inhibition. Together, these findings establish macropinocytosis as a key endocytic mechanism responsible for Lp(a) uptake and reveal that serotonin and antidepressants are important regulators of Lp(a) cell surface binding and uptake.

## Results

### Lp(a) uptake is mediated by macropinocytosis.

To first establish if Lp(a) uptake occurs via macropinocytosis, we investigated the requirement of

extracellular calcium for Lp(a) uptake into HepG2 liver cells. Extracellular calcium was depleted from the cellular media using 2.5 mM EGTA for 1 hour prior to Lp(a) addition. Lp(a) was added to HepG2 cells for 1 hour following which cells were fixed, permeabilised and Lp(a) detected. To quantify Lp(a) endocytosis, cells were imaged by confocal microscopy using identical settings within the independent experiment and image threshold applied to remove Lp(a) signal at the plasma membrane for specific identification of endosomal Lp(a) vesicles (Figure S1). Image quantification confirmed that Lp(a) uptake strictly requires extracellular calcium, with EGTA almost completely abolishing Lp(a) uptake (Figure 1A,B).

To confirm that macropinocytosis was responsible for Lp(a) uptake, we utilised the widely used macropinocytosis inhibitor, the amiloride analogue 5-(N-Ethyl-N-isopropyl)amiloride (EIPA)[28]. While EIPA predominantly inhibits macropinocytosis, it is also capable of inhibiting fast endophilin mediated endocytosis [21]. Fast endophilin mediated endocytosis strictly requires growth factors present in serum[21,22] therefore to minimise any potential contribution of this alternate endocytic pathway, all experiments were performed in serum free media following a minimum of 1 hour serum starvation. EIPA treatment in serum free media lead to robust inhibition of Lp(a) uptake (Figure 1C,D) confirming macropinocytosis is an important endocytic mechanism for Lp(a) internalisation.

Macropinocytosis also represents an important endocytic uptake mechanism for native LDL in macrophages during atherogenesis[30,31], although macropinocytosis of native LDL has not been documented in the liver or HepG2 cells. We sought to exclude a contribution of the LDL moiety of Lp(a) to Lp(a) macropinocytosis by specifically investigating the apo(a) protein component. HEK923 cells were transfected with an apo(a)-cDNA construct fused to the fluorescent protein, mScarlet. Cell media was collected 4 days post transfection, cell debris pelleted and apo(a)-mScarlet concentrated by centrifugation of the media in a 100 kDa molecular weight cut off spin column. Concentrated apo(a)-mScarlet did not contain any apoB (Figure S2A) and was capable of forming Lp(a) when incubated with plasma from a human apoB expressing mouse (Figure S2B). We concluded that concentrated apo(a)-mScarlet was an appropriate system for probing the function of apo(a) alone. Inhibition of macropinocytosis with EIPA in serum free media also inhibited apo(a)-mScarlet uptake (Figure 1E,F). Lp(a) macropinocytosis is therefore likely mediated by the apo(a) component of Lp(a).

We next sought to confirm that Lp(a) uptake by macropinocytosis was not specific to HepG2 cells, but rather represents a broad endocytic mechanism of Lp(a) internalisation. We differentiated THP-1 monocytes into macrophages using PMA[32]. EGTA (Figure 2A,B) and amiloride (Figure 2C,D) inhibited Lp(a) uptake, supporting Lp(a) uptake being regulated by macropinocytosis. To provide additional confirmation that Lp(a) uptake is regulated by macropinocytosis we used the tricyclic antidepressant imipramine, which has been recently identified as a macropinocytosis inhibitor in macrophages[29]. Imipramine inhibited both Lp(a) uptake and 70 kDa dextran uptake (Figure 2E-H), providing further confirmation that macropinocytosis is responsible for Lp(a) uptake.

**Antidepressants are modulators of Lp(a) uptake.**

Antidepressants have been long observed to increase circulating HDL and LDL levels[33–37]. As imipramine inhibited Lp(a) uptake in THP-1 macrophages, we tested whether clinically utilised SSRI antidepressants could modulate Lp(a) uptake. The SSRIs citalopram, fluoxetine and sertraline all inhibited Lp(a) and dextran uptake into differentiated THP-1 macrophages following overnight treatment (Figure 2G-H), indicating SSRIs reduce Lp(a) uptake into macrophages by inhibiting macropinocytosis.

We next evaluated the effects of antidepressants in HepG2 cells. Unexpectedly, imipramine treatment stimulated Lp(a) uptake in HepG2 cells in a concentration-dependent manner (Figure 3A,B). Treatment of HepG2 cells with 20 µM imipramine overnight lead to an average ~280% increase in Lp(a) uptake across seven independent experiments (Figure 3C), strongly indicating that imipramine is a robust stimulator of Lp(a) uptake into liver cells.

Similar to imipramine, overnight treatment with the SSRI citalopram induced robust, concentration-dependent increases in Lp(a) uptake (Figure 3D-F). The SSRIs fluoxetine and sertraline were applied for 2 hours prior to Lp(a) uptake as overnight treatments were not well tolerated in HepG2 cells. Fluoxetine did not alter Lp(a) uptake (Figure 3G-I). In contrast, sertraline induced a concentration-dependent inhibition of Lp(a) uptake (Figure 3J-L). Unexpectedly, dextran uptake was not increased with imipramine or citalopram treatment and was inhibited by fluoxetine and sertraline treatments (Figure 3M,N). Imipramine and citalopram therefore do not stimulate Lp(a) uptake by specifically inducing macropinocytosis in liver cells.

We explored the discordant results between macrophage and liver cells with respect to the effects of imipramine and citalopram. Both drugs are previously established de-differentiators of THP-1 macrophages, with corresponding functional reductions in phagocytosis[38]. Given the similarities between phagocytosis and macropinocytosis[39], we tested dextran and Lp(a) uptake in undifferentiated versus differentiated THP-1 cells. Undifferentiated THP-1 cells exhibited almost no uptake of dextran or Lp(a), with differentiation inducing significant increases in uptake of both (Figure S3 A-D). These results show that like phagocytosis, macropinocytosis can be upregulated in differentiated macrophages, suggesting that imipramine and citalopram could inhibit Lp(a) uptake in macrophages by dedifferentiation, an effect not reported in liver cells. With respect to the inhibitory effect of sertraline on both cell lines, potent off target inhibitory effects on the mediator of endosome scission, dynamin, have been observed for sertraline but not for citalopram or imipramine[40]. Sertraline inhibition of dynamin prevents endocytosis of the *bona fide* dynamin-dependent cargo transferrin[41]. While macropinocytosis is conflictingly described as dynamin-dependent and dynamin-independent[27,42], constitutive macropinocytosis (as opposed to growth factor activated macropinocytosis) is dependent on dynamin in a wide range of cell types including primary rat hepatocytes[42,43]. Given the hepatic origin of the HepG2 cell line and the exclusion of serum in our experiments, constitutive macropinocytosis is the process likely active in our experimental conditions. We therefore hypothesised that the inhibitory effects of sertraline on Lp(a) macropinocytosis were due to inhibition of dynamin-dependent uptake processes. To test this, we quantified the uptake of transferrin, Lp(a) and dextran in the presence or absence of sertraline. As expected, sertraline inhibited the uptake of the dynamin-dependent cargo transferrin (Figure S3 E,F), as well as Lp(a) and dextran (Figure S3 G-J), consistent with the inhibitory effects of sertraline on macropinocytosis being due to dynamin inhibition.

**Imipramine and citalopram stimulate Lp(a) binding to the cell surface.**

We next sought to understand how imipramine and citalopram stimulated Lp(a) uptake in liver cells. We hypothesised that imipramine or citalopram may be stimulating Lp(a) uptake by increasing Lp(a) binding to the plasma membrane, which could then allow higher levels of engulfment without directly stimulating macropinocytic processes. To test this, we performed experiments specifically investigating Lp(a) and dextran bound to the cell surface. HepG2 cells were treated with imipramine or citalopram overnight, cooled to prevent endocytic uptake occurring and the amount of Lp(a) or dextran-TRITC bound was quantified. Lp(a) was detected by incubation of the LPA4 antibody and corresponding secondary antibody to chilled cells, while dextran was detected directly. Consistent with imipramine and citalopram stimulating Lp(a) surface binding, Lp(a) levels on the cell surface were increased following treatment in HepG2 cells (Figure 4A,B). Conversely, dextran surface binding was unaltered by imipramine and citalopram treatment (Figure 4C,D), confirming that the increase in Lp(a) macropinocytosis induced by imipramine and citalopram is due to specific, enhanced Lp(a) binding to the plasma membrane.

To further confirm the effect of citalopram on HepG2 cells, cells were citalopram treated overnight, glutaraldehyde-fixed and imaged using scanning electron microscopy. Citalopram treatment lead to formation of distinct protrusions and membrane ruffles projecting from the plasma membrane (Figure 4E,F, white arrows). These plasma membrane alterations are consistent with the plasma membrane remodelling consistently observed in macropinocytosis[44], and the increased microvilli observed in HepG2 cells that facilitate immune cell adhesion to the plasma membrane[45]. The effects of citalopram on the cell are consistent with the facilitation of increased adhesion of Lp(a) and apo(a) to the plasma membrane and subsequent macropinocytic engulfment.

To confirm that apo(a) is the predominant mediator of Lp(a) uptake, we repeated surface binding and uptake results using apo(a)-mScarlet. Imipramine and citalopram induced increases in apo(a) surface binding to HepG2 cells (mean surface intensity of 461850 for imipramine, 432856 for citalopram vs. 174446 for vehicle control) in each of 4 independent experiments, however this did not reach statistical significance (Figure S4A,B). Imipramine and citalopram both induced robust, significant increases in apo(a)-mScarlet uptake into HepG2 cells (Figure S4C-E), indicating that the increased surface binding observed is biologically relevant. Together, these results indicate apo(a) mediates the plasma membrane binding and subsequent uptake of Lp(a).

**Serotonin enhances Lp(a) cell surface binding and macropinocytosis**

The primary target of antidepressants is the serotonin transporter. Serotonin transporter inhibition prevents serotonin uptake from the extracellular space[46], leading to elevated extracellular serotonin levels. Interestingly, a recent study found addition of exogenous serotonin to

cells enhances transferrin cell surface binding and subsequent endocytosis by altering the physical properties of the plasma membrane independent of serotonin receptors or transporter[47]. HepG2 cells only express minimal levels of the serotonin receptors 1A and 1D and the highest level of the serotonin transporter of any human cell line (Human Protein Atlas[48]). Imipramine and citalopram treatment may enhance Lp(a) surface binding by inhibiting the serotonin transporter, allowing accumulation of extracellular serotonin and inducing membrane changes as observed by Dey et al[47].

To test whether serotonin alone enhanced Lp(a) binding to the plasma membrane, we treated HepG2 cells with serotonin overnight, prior to Lp(a) addition to cells incubated on ice. Treatment with 0.5 mM serotonin resulted in a significant increase (~230%) in Lp(a) binding to the cell surface (Figure 5A,B). Consistent with increased Lp(a) surface binding, treatment with 0.5 mM serotonin induced a comparable increase in Lp(a) uptake (~260%, Figure 5C-E). Interestingly, co-treatment of cells with serotonin and the macropinocytosis inhibitor EIPA abolished the effect of serotonin on Lp(a) (Figure 5D,E), indicating that serotonin-enhanced surface binding still requires macropinocytosis for cargo uptake. In keeping with the specific effects of imipramine and citalopram on Lp(a) uptake, treatment of HepG2 cells with serotonin resulted in no significant changes in dextran binding to the cell surface (Figure 5F,G). Further, as would be expected with no changes in surface binding, no significant changes were observed in dextran uptake into the cell with serotonin treatment. This data therefore demonstrated that serotonin specifically increases Lp(a) surface binding to HepG2 cells that translates into increased Lp(a) uptake *via* macropinocytosis.

**Imipramine and citalopram stimulate Lp(a) and apo(a) recycling.**

We have previously reported that following internalisation, the apo(a) protein component of Lp(a) is recycled back into the extracellular environment while the LDL component is targeted to the lysosome[13]. We thus tested the effects of imipramine and citalopram on the endosomal sorting of Lp(a) and apo(a) into recycling compartments of the cell.

Lp(a) was added to HepG2 cells for 30 or 120 minutes following overnight imipramine/citalopram treatment, cells fixed, permeabilised and co-stained for Lp(a) and Rab11 (recycling endosomes), Rab7 (late endosomes) or LAMP1 (lysosomes). Cells were then imaged by confocal microscopy and co-localisation between Lp(a) and endosomal compartment markers determined by overlap of threshold-defined endosomal signals between channels to exclude contribution of plasma membrane signal.

After 30 minutes of incubation, Lp(a) co-localisation with Rab11 was significantly increased with imipramine and citalopram treatments compared to vehicle control (Figure 6A,E). No significant difference in Lp(a) and Rab11 co-localisation was observed between vehicle control and imipramine/citalopram following 120 minutes of Lp(a) incubation (Figure 6B,E). No significant difference between vehicle control and imipramine/citalopram treated cells was observed in Lp(a) co-localisation with either Rab7 (Figure 6C,D,F) or LAMP1 (Figure S5 A-C) at any timepoint. Apo(a) co-localisation with Rab11 was significantly increased by citalopram treatment compared to vehicle at both the 30 and 120-minute timepoints, while imipramine did not induce significant changes to apo(a) colocalisation (Figure S5A-C). These results are concordant with our previous study showing Lp(a) is sorted primary to recycling and not degradative compartments within the cell[13] and indicates imipramine and citalopram promote apo(a) delivery into $Rab11^{+}$ recycling endosomes.

We next tested the functional impact of the antidepressant-induced alterations to Lp(a) and apo(a) recycling by Western blot. Lp(a) or apo(a) were added to vehicle, imipramine or citalopram treated HepG2 cells for 2 hours in serum free media. Lp(a)/apo(a) containing media was then removed, cells washed, and fresh media added. This media was then immediately collected, and cells lysed for baseline uptake and recycling measurements, or incubated in the fresh media for 2 or 6 hours to assess Lp(a)/apo(a) retention within the cell and recycling to the media. Both imipramine and citalopram treatment significantly increased the Lp(a) signal within the cell across all time points compared to the vehicle control (Figure 7A,B). Imipramine and citalopram treatments also significantly increased Lp(a) recycling into the cellular media over time compared to the vehicle control (Figure 7C,D), consistent with the observed increase in co-localisation with Rab11 induced by these antidepressants (Figure 6A,E).

While citalopram treatment significantly increased apo(a) signal within the cell across all time points compared to the vehicle control, imipramine treatment led to an increase in apo(a) signal approaching statistical significance ($p=0.0515$) (Figure 7D,E). Citalopram treatment alone led to a significant increase in apo(a) recycling to the cellular media (Figure 7I,J), consistent

with the citalopram-specific increase in apo(a) colocalisation with Rab11 observed (Figure S6). Together, these results indicate that imipramine and citalopram increase Lp(a) and apo(a) uptake into the cell, increase their delivery to cellular recycling compartments and subsequent stimulate recycling into the cellular media.

## Discussion

Endocytosis is the central regulator of lipoprotein clearance from circulation[49]. LDL uptake via the LDLR is the most well characterised pathway of lipoprotein endocytosis[50,51]. In contrast, the endocytic mechanisms mediating the uptake of the LDL-like Lp(a) molecule are unknown[17,49]. In this study we have established that Lp(a) uptake occurs via the fluid-phase endocytic mechanism, macropinocytosis (Figure 8). In defining this process, we have found that Lp(a) uptake is: (1) mediated by the apo(a) protein component, (2) dependent on extracellular calcium, (3) inhibited by amiloride/EIPA, and (4) occurs in a manner analogous to the canonical marker of macropinocytosis, 70 kDa dextran in liver cells and macrophages. In pharmacologically defining the macropinocytic uptake of Lp(a), we discovered that common antidepressants exert complex effects on Lp(a) uptake (Figure 8). The tricyclic antidepressant, imipramine and the SSRIs, citalopram, sertraline and fluoxetine all inhibit Lp(a) uptake by macropinocytosis in THP-1 macrophages, likely due to their de-differentiation or dynamin inhibitory effects on these cells[38,40]. In HepG2 liver cells, imipramine and citalopram stimulated Lp(a) uptake by increasing Lp(a) binding to the cell surface. Serotonin similarly increased Lp(a) cell surface binding and uptake *via* macropinocytosis, indicating the effects of imipramine and citalopram on Lp(a) are serotonin-dependant. Functionally, antidepressant-stimulated (imipramine and citalopram) Lp(a) uptake resulted in increased Lp(a) delivery to the recycling compartment of the cell, but not to degradative compartments, increasing recycling of Lp(a)-derived apo(a) protein into the cellular media.

Lp(a) uptake via macropinocytosis represents a critical paradigm shift in understanding Lp(a) clearance from circulation. Other modes of endocytosis such as clathrin-dependent endocytosis or fast endophilin mediated endocytosis occur following ligand: receptor binding[18,22]. In contrast, macropinocytosis occurs following extensive membrane remodelling to form a macropinocytic cup in which cargoes are engulfed[52]. Imipramine, citalopram and serotonin enhanced binding of Lp(a) to the plasma membrane suggests that membrane anchoring provides a further layer of regulation upon Lp(a) uptake. The apo(a) homologue, plasminogen, has been shown to bind to cell surface actin[53], before it is endocytosed into the cell[54]. Similar to this, older Lp(a) studies have reported that Lp(a) can bind to the cell surface via interaction with actin[55]. Moreover, Lp(a)[56] and serotonin[57] have each been shown to stimulate actin remodelling in endothelial cells. The interplay between Lp(a) and serotonin is likely to extend to modification of actin within the cell to facilitate Lp(a) surface binding and uptake.

The finding that Lp(a) enters the cell via macropinocytosis is compelling as there has been many competing studies that have not agreed on a clear receptor-mediated process driving Lp(a) uptake. At least twelve receptors have been proposed to date to mediate Lp(a) uptake into the cell, yet no receptor has been shown to play a definitive role in mediating this uptake[17]. Lp(a) binds to receptors such as the plasminogen receptor $PlgR_{KT}$ and SR-BI[13,58] which have been demonstrated to bind other ligands (plasminogen, HDL respectively) to the plasma membrane while not inducing receptor-mediated endocytosis[59,60]. We propose that for at least a subset of receptors implicated in Lp(a) uptake, these receptors act not as mediators of Lp(a) internalisation into the cell, but rather as membrane anchors immobilising Lp(a) to the plasma membrane and allowing macropinocytic engulfment to occur.

Links between depression and increased atherosclerotic cardiovascular disease development have long been observed[61,62]. Circulating Lp(a) levels are increasingly recognised to be elevated in patients with depression, an increase that correlates with unfavourable cardiovascular outcomes[63–66]. Our data could provide a mechanistic explanation of elevated Lp(a) levels in patients with depression. Plasma serotonin levels are often decreased in patients with depression[67–69]. Serotonin has been recently discovered to be a regulator of cargo binding to the plasma membrane[47]. Consistent with this, we found that serotonin increased plasma membrane binding of Lp(a) to the cell surface, and this enhanced binding subsequently increased Lp(a) uptake

by macropinocytosis. Taken together, this indicates that reduced plasma serotonin could be governing decreased Lp(a) cell surface binding and uptake in patients with depression, thus leading to increased circulating Lp(a) levels. A double-blinded interventional study has shown that treatment with the SSRI paroxetine did in fact decrease circulating Lp(a) levels[70]. In light of our data, we hypothesise that patients with depression and high Lp(a) levels may benefit from treatment with an SSRI such as citalopram which would likely reduce Lp(a) levels in circulation by boosting cellular uptake. Conversely sertraline may not be suitable since it may have the opposite effect of increasing circulating Lp(a) levels by inhibiting cellular uptake.

Imipramine and citalopram increased Lp(a) uptake in liver cells, where Lp(a) catabolism is primarily proposed to occur[71]. Both drugs also promoted apo(a) recycling after Lp(a) uptake. The function of apo(a) recycling has been reported in the literature though its function is unclear. We have previously found that after Lp(a) uptake into the cell, the apo(a) protein component is removed from the LDL-like component and rather than undergoing lysosomal or proteasomal degradation is re-secreted to the extracellular space[13]. Free apo(a) has been long identified in circulation and urine in consistently proteolysed forms in healthy[72,73] and in nephrotic syndrome patients[74] that is consistent with extracellular matrix metalloproteinase degradation of free apo(a) in the extracellular environment *in vitro* and in mouse plasma *in vivo*[73,75]. Together, these studies indicate that when apo(a) is free in the extracellular environment it may be susceptible to cleavage by extracellular proteases and then removed from the body in the urine. We hypothesise that recycling serves as a mechanism to remove the LDL-like component of Lp(a), releasing free apo(a) into circulation for proteolysis and excretion from the body. Our finding that imipramine and citalopram stimulate apo(a) recycling indicates these drugs may lead to not only decreased circulating Lp(a) levels *in vivo* but also increased apo(a) degradation.

Questions remain from our current study that need to be addressed to better understand the effects of serotonin and antidepressants on Lp(a) uptake. This study was entirely *in vitro* in nature. While we have identified that cell surface binding is an important mediator of Lp(a) uptake, and serotonin boosts this binding, this study did not evaluate if receptors previously implicated in Lp(a) uptake are involved in this process, or if this process is predominantly mediated by the effects of serotonin in the plasma membrane. Future studies evaluating the plasma membrane binding of Lp(a) in cells depleted of these receptors and determining if serotonin and antidepressants increase their expression will prove highly informative as to how Lp(a) surface binding is regulated.

In conclusion, our data show that macropinocytosis regulates Lp(a) uptake, indicating that modulation of macropinocytosis may be a potential therapeutic avenue for reducing Lp(a) levels. We provide an *in vitro* link between studies correlating depression with increased circulating Lp(a) levels *via* serotonin enhancement of Lp(a) macropinocytosis. Our study strongly indicates that antidepressants, especially the SSRI citalopram, should be investigated pre-clinically and clinically for their effects on Lp(a) levels in circulation. The benefit of identifying specific SSRIs capable of reducing Lp(a) levels *in vivo* are clear as depression is increasingly linked with higher Lp(a) levels[63–66]. Depression sufferers are less likely to adhere to treatments for co-morbidities such as cardiovascular disease[76–78]. SSRIs that reduce Lp(a) levels in depression sufferers would allow treatment of their mental health and Lp(a)-induced atherosclerotic burden with a single medicine, improving their quality of life and cardiovascular health with the maximum likelihood of compliance.

## Acknowledgements

This research was supported by project grants from the Royal Society of New Zealand (Marsden Fund 17-UOO-081) and the Health Research Council of New Zealand (18/207).

## Author contributions

ND, GMIR, HS, GM and NK performed the experiments. MW recruited Otago LPA cohort subjects, MR purified the Lp(a). GMIR, ND and NA analysed the data. GMIR, ND and SPAM prepared the figures and wrote the manuscript. ND prepared the schematic. GR, ND and SPAM supervised the students. GR and SPAM conceived of the study.

## Declaration of Interests

All authors declare no competing interests.

## Methods

### *Resource Availability*

#### *Lead contact*

Further information and requests for resources and reagents should be directed to and will be fulfilled by the Lead Contact, Professor Sally PA McCormick (sally.mccormick@otago.ac.nz).

#### *Data and Code Availability*

The raw confocal imaging data has been deposited into the FigShare repository.
FIJI Macros are available upon request.

### *Experimental Model and Subject Details*

#### *Cell culture*

Cells were grown at 37°C in a 5% $CO_2$ humidified incubator. HepG2 cells (ATCC, CVCL-2205) and HEK293 cells (ATCC, CVCL_0045) were cultured in DMEM with 10% FBS, 100 u/ml penicillin, 100µg/ml streptomycin, and 0.25 mg/mL amphotericin B. THP-I cells (ATCC, CVCL_0006) were cultured in RPMI with 10% FBS, 100 u/ml penicillin, 100µg/ml streptomycin, and 0.25 mg/mL amphotericin B. THP-I cells were differentiated for 72 hours prior to use with 100 nM Phorbol 12-myristate 13-acetate (PMA) (Sigma-Aldrich).

#### *Lp(a) enrichment from patient samples*

Lp(a) was isolated from plasma samples from healthy individuals from the Otago LPA cohort [79] with Lp(a) levels >50 mg/dL (equivalent to 108 nmol/L using a conversion factor of 2.15). Individual samples used for isolation had apo(a) isoform sizes ranging from 17-20 with a predominant apo(a) isoform size of 19. 100 µg (HepG2) or 200 µg (THP-I) by total protein concentration of enriched Lp(a) was used per well. Purified Lp(a) protein levels were quantified using the Qubit Protein Assay Kit (Thermo Fisher Scientific).

#### *Ethical Approval*

Ethical approval for the samples used in this study was granted by the Lower Regional South Ethics Committee (LRS/12/01/005).

### *Method Details*

#### *Drug treatments*

For serotonin, imipramine and citalopram treatments, cells were treated overnight prior to the experiment. Two hours before addition of Lp(a)/apo(a), cells were transferred into serum-free media and new serotonin/imipramine/citalopram added. For sertraline and fluoxetine treatments in HepG2 cells, cells were transferred into serum-free media two hours prior to Lp(a)/apo(a) addition. For sertraline and fluoxetine treatments in THP-I cells, cells were treated overnight prior to the experiment. Two hours before addition of Lp(a)/apo(a), cells were transferred into serum-free media and new sertraline/fluoxetine added. For amiloride/EIPA/EGTA treatments, cells were transferred into serum-free media one hour prior to Lp(a)/apo(a) addition.

#### *Immunofluorescence staining*

Cells were fixed with 4% paraformaldehyde for 15 minutes at 37°C in a humidified incubator. Cells were then washed with PBS and blocked with 3% goat serum. The antibodies used in this study were: anti-apolipoprotein(a) antibody, clone LPA4 (Millipore), rabbit monoclonal anti-Lp(a) antibody (Abcam), goat polyclonal anti-Lp(a) antibody (WAKO), rabbit monoclonal anti-Rab7 (Abcam), rabbit anti-LAMP1 (Cell Signaling Technolgies) and rabbit anti-Rab11 (Cell Signaling Technologies). The secondary antibodies include goat anti-rabbit Alexa Fluor 594, anti-mouse Alexa Fluor 488, and anti-rabbit Alexa Fluor 594 (ThermoFisher Scientific, 1:1000). Slides were mounted with ProLong™ antifade mounting medium (Invitrogen).

#### *Confocal imaging*

All coverslips were imaged on an Olympus FV1000/1200/3000 confocal microscope using 405, 488 and 561 nm laser lines with a 60x, NA 1.4 oil immersion lens. Within each experiment, images from each coverslip were captured using identical laser power, gain, offset and PMT (FV1000/1200)/GaAsP(FV3000) detector voltage. The maximum field of view was captured at a pixel size of ~125-135 nm.

#### *Electron microscopy*

All the steps were carried out in a PELCO Biowave microwave processor (TedPellaInc., Redding, CA, USA). PFA fixed samples on coverslips were first re- fixed in 2.5% glutaraldehyde in 0.1 M sodium cacodylate buffer, washed with 0.1 M sodium cacodylate buffer followed by post-fixation with 1% OsO4 (osmium tetroxide) (ProScitech) in cacodylate buffer. Following buffer and water washes, fixed samples were serially dehydrated in increasing percentages of ethanol and finally dried in a critical point drier. Dried samples were mounted on stubs, sputter coated with platinum and imaged using a FEI Nova NanoSEM 230 at 5 kV.

#### *Immunoblotting*

Cultured cells were washed twice with ice cold PBS and lysed in radioimmune precipitation assay (RIPA) buffer containing 20 mm Tris HCl, pH 7.5, 150 mm NaCl, 1 mm EDTA, 1 mm EGTA, 1% Triton X-100, 2.5 mm sodium pyrophosphate, 1 mm β-glycerophosphate, 1 mm Na3VO4, 1 mm NaF, and 1× protease inhibitor mixture (Roche Applied Science). After incubation on ice for 10 min, cell lysates were subjected to

centrifugation at 15,000 rpm for 10 min. 60 mg of total lysates were subjected to 4-12% sodium dodecyl sulfate polyacrylamide gradient gel electrophoresis and transferred onto membranes. Membranes were blocked in 5% skim milk buffer in PBS with 0.1% Triton-X for 1 h and incubated with primary antibodies at 4°C overnight followed by probing with fluorescence labelled secondary antibodies. Proteins were detected with the Odyssey Infrared Imaging System (LI-COR Biosciences). Densitometry was analysed with FIJI/ImageJ software.

### *Apo(a) expression and concentration*

Apo(a)-mScarlet was transfected into HEK293 cells using Lipofectamine 3000. 4 days post transfection, cell media was collected, cooled and centrifuged at 3000g to pellet cellular debris. Media was then transferred into a 20 mL, 100 kDa MW cutoff centrifuge tube (Thermo Fisher Scientific) and centrifuged at 3000g at 4°C until media volume was 5x concentrated. Concentrated media was frozen until used.

### *Immunoprecipitation of cell media for recycling experiments*

To detect the secretion of Lp(a) particles into culture media following incubation with the purified lipoprotein, culture media was collected and immunoprecipitated prior to analysis by western blot. Following 2h incubation with Lp(a) in a humidified 37°C incubator to foster maximal uptake of the lipoprotein, culture media was removed, cells washed 5x with PBS, and fresh media added to cells. Media was harvested from 0-6h post-treatment and incubated with a solution of polyclonal Lp(a) antibody (WAKO) immobilised on Protein G magnetic beads (Thermo Fisher Scientific). Lp(a) was immunoprecipitated from the media overnight at 4°C and eluted under reducing conditions. Samples were then subjected to western blotting using the LPA4 antibody.

## ***Quantification and Statistical Analysis***

### *Image Quantification*

Images were quantified using FIJI [80]. Custom macros were created for endosome identification and overlap analysis. For endosome identification, a single intensity-based threshold per experiment was used to identify Lp(a)/apo(a) endosomes and nuclei. For overlap analysis, one intensity-based threshold was used to identify Lp(a)/apo(a) endosomes, and another used to identify Rab7/11/LAMP1 compartments. The same threshold was used for each image in a single experiment. The threshold was used to generate a mask for each channel, and the Lp(a)/apo(a) mask subtracted from the inverted Rab7/11/LAMP1 mask to generate an overlap mask of Lp(a)/apo(a) present in the Rab7/11/LAMP1 compartment. The number of Lp(a)/apo(a) endosomes in the overlap mask was quantified and divided by the total number of Lp(a)/apo(a) endosomes to determine the percentage of total Lp(a)/apo(a) endosomes overlapping with Rab7/11/LAMP1 compartments.

### *Data Representation and Statistical analysis*

Data are expressed as means of independent experiments +/- SEM. Statistical analyses were performed with Prism Software version 8 (GraphPad Software).

## ***Resources Table***

| REAGENT or RESOURCE | SOURCE | IDENTIFIER |
|---|---|---|
| **Antibodies** | | |
| Rabbit anti-LAMP1 | Cell Signaling Technology | Cat# 9091; RRID: AB_2687579 |
| Anti-Apolipoprotein(a) antibody, clone LPA4 | Millipore | Cat#MABS1284 |
| Goat polyclonal anti-Lp(a) antibody | Wako Pure Chemical Industries (Osaka, Japan) | Cat# |
| Rabbit monoclonal anti-Rab7 [EPR7589] | Abcam | Cat#ab137029; RRID: AB_2629474 |
| Rabbit anti-Rab11 | Cell Signaling Technology | Cat# 5589; RRID: AB_10693925 |
| Rabbit monoclonal anti-Lp(a) antibody | Abcam | Cat# ab208184 |
| Mouse monoclonal anti-apoB antibody clone 1D1 | | |
| Donkey anti-Mouse IgG (H+L) Highly Cross-Adsorbed Secondary Antibody, Alexa Fluor 488 | Thermo Fisher Scientific | Cat# A-21202, RRID:AB_141607 |
| Donkey anti-Mouse IgG (H+L) Highly Cross-Adsorbed Secondary Antibody, Alexa Fluor 594 | Thermo Fisher Scientific | Cat# A-21203, RRID:AB_141633 |
| Donkey anti-Rabbit IgG (H+L) Highly Cross-Adsorbed Secondary Antibody, Alexa Fluor 488 | Thermo Fisher Scientific | Cat# A-21206, RRID:AB_2535792 |
| Donkey anti-Rabbit IgG (H+L) Highly Cross-Adsorbed Secondary Antibody, Alexa Fluor 594 | Thermo Fisher Scientific | Cat# A-21207, RRID:AB_141637 |
| **Biological Samples** | | |

| | | |
|---|---|---|
| Purified human Lp(a) | | |
| **Chemicals, Peptides, and Recombinant Proteins** | | |
| Phosphate buffered saline, pH 7.4 | Gibco | Cat#10010023 |
| DMEM, high glucose | Gibco | Cat#11965092 |
| RPMI 1640 medium | Gibco | Cat#11875119 |
| Fetal Bovine Serum, qualified, New Zealand | Gibco | Cat#10091155 |
| Penicillin-Streptomycin (10,000 U/mL) | Gibco | Cat#15140122 |
| Amphotericin B | Gibco | Cat#15290018 |
| TrypLE™ Express Enzyme (1X), no phenol red | Gibco | Cat#12604021 |
| Dextran, Tetramethylrhodamine, 70,000 MW, Lysine Fixable | Invitrogen | Cat#D1818 |
| Dextran, Oregon Green 488; 70,000 MW, Anionic, Lysine Fixable | Invitrogen | Cat#D7173 |
| 5-(N-Ethyl-N-isopropyl)amiloride | Sigma-Aldrich | Cat#A3085 |
| Amiloride hydrochloride hydrate | Sigma-Aldrich | Cat#A7410 |
| Ethylene glycol-bis(2-aminoethylether)-N,N,N′,N′-tetraacetic acid | Sigma-Aldrich | Cat#E3889 |
| ProLong™ antifade mounting reagent | Invitrogen | Cat#P36934 |
| Triton-X100 | Bio-Rad Laboratories | Cat#1610407 |
| Tween-20 | Bio-Rad Laboratories | Cat#1706531 |
| TEMED | Bio-Rad Laboratories | Cat#1610801 |
| Precision Plus Protein™ All Blue Prestained Protein Standards | Bio-Rad Laboratories | Cat#1610373 |
| Bolt™ 4 to 12%, Bis-Tris, 1.0 mm, Mini Protein Gel, 10-well | Invitrogen | Cat#NW04120BOX |
| Imipramine hydrochloride | Sigma-Aldrich | Cat#I7379 |
| Sertraline tablets 50 mg as hydrochloride | Teva Pharmaceutical Industries Limited | |
| Fluoxetine tablets 20 mg as hydrochloride | Teva Pharmaceutical Industries Limited | |
| Citalopram tablets 20 mg as hydrobromide | PSM Healthcare Limited | |
| Serotonin hydrochloride (5-Hydroxytryptamine) | Abcam | Cat#ab120528 |
| Phorbol 12-myristate 13-acetate | Sigma-Aldrich | Cat#P1585 |
| Paraformaldehyde | Sigma-Aldrich | Cat#P6148 |
| Goat Serum, New Zealand origin | Sigma-Aldrich | Cat#16210064 |
| Plasminogen from human plasma | Athens Research and Technology | Cat#16-16-161200 |
| Alexa Fluor 488 Microscale Protein labelling kit | Life Technologies | Cat#A30006 |
| Qubit Protein Assay Kit | Thermo Fisher Scientific | Cat#Q33211 |
| Pierce Protein Concentrator PES, 100K MWCO, 5-20 mL | Thermo Fisher Scientific | Cat#88532 |
| Lipofectamine 3000 | Life Technologies | Cat#L3000015 |
| **Deposited Data** | | |
| Figshare | | |
| **Experimental Models: Cell Lines** | | |
| HepG2 | ATCC | ATCC Cat# HB-8065, RRID:CVCL_0027 |
| THP-1 | ATCC | ATCC Cat# TIB-202, RRID:CVCL_0006 |
| HEK293 | ATCC | ATCC Cat# CRL-1573, RRID:CVCL_0045 |
| **Recombinant DNA** | | |
| Lipoprotein a (LPA) (NM_005577) Human Tagged ORF Clone | Origene | CAT#RG212070 |
| **Software and Algorithms** | | |
| Prism | Graphpad | RRID:SCR_002798 |
| FIJI | | RRID:SCR_002285 |
| Fluoview FV-10 ASW | Olympus | RRID:SCR_014215 |

## References


1. Boerwinkle, E. *et al.* Apolipoprotein(a) gene accounts for greater than 90% of the variation in plasma lipoprotein(a) concentrations. *J. Clin. Invest.* **90**, 52–60 (1992).
2. Lawn, R. M., Schwartz, K. & Patthy, L. Convergent evolution of apolipoprotein(a) in primates and hedgehog. *Proc. Natl. Acad. Sci. U. S. A.* **94**, 11992–7 (1997).
3. Wilson, D. P. *et al.* Use of Lipoprotein(a) in clinical practice: A biomarker whose time has come. A scientific statement from the National Lipid Association. *J. Clin. Lipidol.* **13**, 374–392 (2019).
4. Patel, A. P. *et al.* Lp(a) (Lipoprotein[a]) Concentrations and Incident Atherosclerotic Cardiovascular Disease. *Arterioscler. Thromb. Vasc. Biol.* 1–10 (2020) doi:10.1161/ATVBAHA.120.315291.
5. Langsted, A. & Nordestgaard, B. G. Lipoprotein(a): Is It More, Less or Equal to LDL as a Causal Factor for Cardiovascular Disease and Mortality? *Curr. Opin. Lipidol.* **31**, 125–131 (2020).
6. Lippi, G., Favaloro, E. J. & Sanchis-Gomar, F. Antisense lipoprotein[a] therapy: State-of-the-art and future perspectives. *European Journal of Internal Medicine* vol. 76 8–13 (2020).
7. Chaudhary, R., Garg, J., Shah, N. & Sumner, A. PCSK9 inhibitors: A new era of lipid lowering therapy. *World J. Cardiol.* **9**, 76 (2017).
8. Hofmann, S. L. *et al.* Overexpression of human low density lipoprotein receptors leads to accelerated catabolism of Lp ( a ) lipoprotein in transgenic mice . Overexpression of Human Low Density Lipoprotein Receptors Leads to Accelerated Catabolism of Lp ( a ) Lipoprotein in Tra. *J. Clin. Invest.* **85**, 1542–1547 (1990).
9. Tam, S. P., Zhang, X. & Koschinsky, M. L. Interaction of a recombinant form of apolipoprotein [ a ] with human fibroblasts and with the human hepatoma cell line HepG2. *J. Lipid Res.* **37**, 518–533 (1996).
10. Floren, C., Albers, J. J. & Bierman, E. L. Pages 636-639 UPTAKE OF Lp ( a ) LIPOPROTEIN BY CULTURED FIBROBLASTS Abbreviations : *Biochem. Biophys. Res. Commun.* 636–639 (1981).
11. Romagnuolo, R. *et al.* Roles of the low density lipoprotein receptor and related receptors in inhibition of lipoprotein ( a ) internalization by proprotein convertase subtilisin / kexin type 9. *PLoS One* **12**, 1–20 (2017).
12. Argraves, K. M. T., Kozarsky, K. F., Fallon, J. T., Harpel, P. C. & Strickland, D. K. The atherogenic lipoprotein Lp(a) is internalized and degraded in a process mediated by the VLDL receptor. *J. Clin. Invest.* **100**, 2170–2181 (1997).
13. Sharma, M., Redpath, G. M., Williams, M. J. A. & McCormick, S. P. A. Recycling of Apolipoprotein(a) After PlgRKT-Mediated Endocytosis of Lipoprotein(a). *Circ. Res.* **120**, 1091–1102 (2017).
14. Chemello, K. *et al.* Lipoprotein(a) Cellular Uptake Ex Vivo and Hepatic Capture In Vivo Is Insensitive to PCSK9 Inhibition With Alirocumab. *JACC Basic to Transl. Sci.* **5**, 549–557 (2020).
15. Reblin, T. *et al.* Cellular uptake of lipoprotein[a] by mouse embryonic fibroblasts via the LDL receptor and the LDL receptor-related protein. *J. Lipid Res.* **38**, 2103–2110 (1997).
16. Rader, D. J. *et al.* The low density lipoprotein receptor is not required for normal catabolism of Lp(a) in humans. *J. Clin. Invest.* **95**, 1403–1408 (1995).
17. McCormick, S. P. A. & Schneider, W. J. Lipoprotein(a) catabolism: a case of multiple receptors. *Pathology* **51**, 155–164 (2019).
18. Redpath, G. M. I., Betzler, V. M., Rossatti, P. & Rossy, J. Membrane Heterogeneity Controls Cellular Endocytic Trafficking. *Frontiers in Cell and Developmental Biology* vol. 8 (2020).
19. Traub, L. M. & Bonifacino, J. S. Cargo recognition in clathrin-mediated endocytosis. *Cold Spring Harb. Perspect. Biol.* **5**, (2013).
20. Haucke, V. Cargo Takes Control of Endocytosis. *Cell* **127**, 35–37 (2006).
21. Boucrot, E. *et al.* Endophilin marks and controls a clathrin-independent endocytic pathway. *Nature* **517**, 460–465 (2015).
22. Casamento, A. & Boucrot, E. Molecular mechanism of Fast Endophilin-Mediated Endocytosis. *Biochem. J.* **477**, 2327–2345 (2020).
23. Canton, J. *et al.* Calcium-sensing receptors signal constitutive macropinocytosis and facilitate the uptake of NOD2 ligands in macrophages. *Nat. Commun.* **7**, 11284 (2016).
24. Lundmark, R. *et al.* The GTPase-Activating Protein GRAF1 Regulates the CLIC/GEEC Endocytic Pathway. *Curr. Biol.* **18**, 1802–1808 (2008).
25. Kumari, S. & Mayor, S. ARF1 is directly involved in dynamin-independent endocytosis. *Nat. Cell Biol.* **10**, 30–41 (2008).
26. Sathe, M. *et al.* Small GTPases and BAR domain proteins regulate branched actin polymerisation for clathrin and dynamin-independent endocytosis. *Nat. Commun.* **9**, 1–16 (2018).
27. Li, L. *et al.* The effect of the size of fluorescent dextran on its endocytic pathway. *Cell Biol. Int.* **39**, 531–539 (2015).
28. Koivusalo, M. *et al.* Amiloride inhibits macropinocytosis by lowering submembranous pH and preventing Rac1 and Cdc42 signaling. *J. Cell Biol.* **188**, 547–563 (2010).
29. Lin, H.-P. P. *et al.* Identification of novel macropinocytosis inhibitors using a rational screen of Food and Drug Administration-approved drugs. *Br. J. Pharmacol.* **175**, 3640–3655 (2018).
30. Kruth, H. S. Receptor-independent fluid-phase pinocytosis mechanisms for induction of foam cell formation with native low-density lipoprotein particles. *Current Opinion in Lipidology* vol. 22 386–393 (2011).
31. Kruth, H. S. *et al.* Macropinocytosis is the endocytic pathway that mediates macrophage foam cell formation with native low density lipoprotein. *J. Biol. Chem.* **280**, 2352–2360 (2005).
32. Daigneault, M., Preston, J. A., Marriott, H. M., Whyte, M. K. B. & Dockrell, D. H. The identification of markers of macrophage differentiation in PMA-stimulated THP-1 cells and monocyte-derived macrophages. *PLoS One* **5**, (2010).
33. Wei, F., Crain, A. L., Whitebird, R. R., Godlevsky, O. V. & Oconnor, P. J. Effects of paroxetine and sertraline on low-density lipoprotein cholesterol: An observational cohort study. *CNS Drugs* **23**, 857–865 (2009).
34. Pan, S. juan *et al.* Fluoxetine induces lipid metabolism abnormalities by acting on the liver in patients and mice with depression. *Acta Pharmacol. Sin.* **39**, 1463–1472 (2018).
35. Rami, M. *et al.* Chronic intake of the selective serotonin reuptake inhibitor fluoxetine enhances atherosclerosis. *Arterioscler. Thromb. Vasc. Biol.* **38**, 1007–1019 (2018).
36. McIntyre, R. S., Soczynka, J. K., Konarski, J. Z. & Kennedy, S. H. The effect of antidepressants on lipid homeostasis: A cardiac safety concern? *Expert Opin. Drug Saf.* **5**, 523–537 (2006).
37. Fjukstad, K. K. *et al.* Metabolic Abnormalities Related to Treatment with Selective Serotonin Reuptake Inhibitors in Patients with Schizophrenia or Bipolar Disorder. *J. Clin. Psychopharmacol.* **36**, 615–620 (2016).
38. Ying, G., Karlsson, H., DePierre, J. W. & Nässberger, L. Tricyclic antidepressants prevent the differentiation of monocytes into macrophage-like cells in vitro. *Cell Biol. Toxicol.* **18**, 425–37 (2002).
39. Mylvaganam, S., Freeman, S. A. & Grinstein, S. The cytoskeleton in phagocytosis and macropinocytosis. *Curr. Biol.* **31**, R619–R632 (2021).
40. Otomo, M. *et al.* Some selective serotonin reuptake inhibitors inhibit dynamin I guanosine triphosphatase (GTPase). *Biol. Pharm. Bull.* **31**, 1489–1495 (2008).
41. Takahashi, K. *et al.* Suppression of dynamin GTPase activity by sertraline leads to inhibition of dynamin-dependent endocytosis. *Biochem. Biophys. Res. Commun.* **391**, 382–387 (2010).
42. Cao, H., Chen, J., Awoniyi, M., Henley, J. R. & McNiven, M. A. Dynamin 2 mediates fluid-phase micropinocytosis in epithelial cells. *J. Cell Sci.* **120**, 4167–4177 (2007).
43. Kolpak, A. L. *et al.* Negative guidance factor-induced macropinocytosis in the growth cone plays a critical role in repulsive axon turning. *J. Neurosci.* **29**, 10488–10498 (2009).
44. Jiang, J., Kolpak, A. L. & Bao, Z. Z. Myosin IIB isoform plays an essential role in the formation of two distinct types of macropinosomes. *Cytoskeleton* **67**, 32–42 (2010).
45. Reglero-Real, N. *et al.* Apicobasal polarity controls lymphocyte adhesion to hepatic epithelial cells. *Cell Rep.* **8**, 1879–1893 (2014).
46. Andersen, J. *et al.* Location of the antidepressant binding site in the serotonin transporter: Importance of Ser-438 in recognition of citalopram and tricyclic antidepressants. *J. Biol. Chem.* **284**, 10276–10284 (2009).
47. Dey, S. *et al.* Altered Membrane Mechanics Provides a Receptor-Independent Pathway for Serotonin Action. *Chem. - A Eur. J.* **27**, 7533–7541 (2021).
48. Thul, P. J. *et al.* A subcellular map of the human proteome. *Science (80-. ).* **356**, (2017).
49. Zanoni, P., Velagapudi, S., Yalcinkaya, M., Rohrer, L. & von Eckardstein, A. Endocytosis of lipoproteins. *Atherosclerosis* vol. 275 273–295 (2018).
50. Goldstein, J. L. & Brown, M. S. The LDL Receptor. *Arterioscler. Thromb. Vasc. Biol.* **29**, 431–438 (2009).
51. Goldstein, J. S. & Brown, M. S. Binding Cultured and Degradation of Low Density Human Fibroblasts Lipoproteins by from. *J. Biol.*

*Chem.* **249**, 5153–5162 (1974).
52. Kerr, M. C. & Teasdale, R. D. Defining macropinocytosis. *Traffic* **10**, 364–371 (2009).
53. Miles, L. A., Andronicos, N. M., Baik, N. & Parmer, R. J. Cell-surface actin binds plasminogen and modulates neurotransmitter release from catecholaminergic cells. *J. Neurosci.* **26**, 13017–13024 (2006).
54. Briens, A. *et al.* Astrocytes regulate the balance between plasminogen activation and plasmin clearance via cell-surface actin. *Cell Discov.* **3**, 1–18 (2017).
55. Dudani, A. K. & Ganz, P. R. Endothelial cell surface actin serves as a binding site for plasminogen, tissue plasminogen activator and lipoprotein(a). *Br. J. Haematol.* **95**, 168–78 (1996).
56. Pellegrino, M. *et al.* The Apolipoprotein ( a ) Component of Lipoprotein ( a ) Stimulates Actin Stress Fiber Formation and Loss of Cell-Cell Contact in Cultured Endothelial Cells *. *J. Biol. Chem.* **279**, 6526–6533 (2004).
57. Alexander, J. S., Hechtman, H. B. & Shepro, D. Serotonin induced actin polymerization and association with cytoskeletal elements in cultured bovine aortic endothelium. *Biochem. Biophys. Res. Commun.* **143**, 152–158 (1987).
58. Yang, X. *et al.* Scavenger receptor-BI is a receptor for lipoprotein ( a ). *J. Lipid Res.* **54**, 2450–2457 (2013).
59. Miles, L. A. *et al.* The Plasminogen Receptor , Plg-R KT , and Macrophage Function. **2012**, (2012).
60. Marques, P. E. *et al.* Multimerization and Retention of the Scavenger Receptor SR-B1 in the Plasma Membrane. *Dev. Cell* **50**, 283-295.e5 (2019).
61. Chávez-Castillo, M. *et al.* Metabolic risk in depression and treatment with selective serotonin reuptake inhibitors: are the metabolic syndrome and an increase in cardiovascular risk unavoidable? *Vessel Plus* **2**, 6 (2018).
62. Hare, D. L., Toukhsati, S. R., Johansson, P. & Jaarsma, T. Depression and cardiovascular disease: A clinical review. *Eur. Heart J.* **35**, 1365–1372 (2014).
63. Bao, J. *et al.* Mental health is correlated with lipoprotein(A) levels in male patients with premature coronary heart disease. *Ann. Palliat. Med.* **10**, 6482–6492 (2021).
64. Hui, N. *et al.* Lipoprotein (a) and the risk of elevated depressive symptoms: The Multi-Ethnic Study of Atherosclerosis. *J. Psychiatr. Res.* **133**, 119–124 (2021).
65. Emanuele, E. *et al.* Elevated plasma levels of lipoprotein(a) in psychiatric patients: A possible contribution to increased vascular risk. *Eur. Psychiatry* **21**, 129–133 (2006).
66. Hamidifard, S., Fakhari, A., Mahboob, S. & Gargari, B. P. Plasma levels of lipoprotein (a) in patients with major depressive disorders. *Psychiatry Res.* **169**, 253–256 (2009).
67. Huang, T. *et al.* Associations of depression status with plasma levels of candidate lipid and amino acid metabolites: a meta-analysis of individual data from three independent samples of US postmenopausal women. *Mol. Psychiatry* (2020) doi:10.1038/s41380-020-00870-9.
68. Trujillo-Hernández, P. E. *et al.* Depressive Symptoms are Associated with low Serotonin Levels in Plasma but are not 5–HTTLPR Genotype Dependent in Older Adults. *Span. J. Psychol.* **24**, (2021).
69. Holck, A. *et al.* Plasma serotonin levels are associated with antidepressant response to SSRIs. *J. Affect. Disord.* **250**, 65–70 (2019).
70. Paslakis, G. *et al.* Treatment with paroxetine, but not amitriptyline, lowers levels of lipoprotein(a) in patients with major depression. *J. Psychopharmacol.* **25**, 1344–1346 (2011).
71. Cain, W. J. *et al.* Lipoprotein [a] is cleared from the plasma primarily by the liver in a process mediated by apolipoprotein [a]. *J. Lipid Res.* **46**, 2681–2691 (2005).
72. Mooser, V. *et al.* Apolipoprotein(a) kringle 4-containing fragments in human urine: Relationship to plasma levels of lipoprotein(a). *J. Clin. Invest.* **97**, 858–864 (1996).
73. Edelstein, C., Shapiro, S. D., Klezovitch, O. & Scanu, A. M. Macrophage metalloelastase, MMP-12, cleaves human apolipoprotein(a) in the linker region between kringles IV-4 and IV-5: Potential relevance to lipoprotein(a) biology. *J. Biol. Chem.* **274**, 10019–10023 (1999).
74. Doucet, C. *et al.* Lipoprotein(a) in the nephrotic syndrome: Molecular analysis of lipoprotein(a) and apolipoprotein(a) fragments in plasma and urine. *J. Am. Soc. Nephrol.* **11**, 507–513 (2000).
75. Edelstein, C., Italia, J. A. & Scanu, A. M. Polymorphonuclear cells isolated from human peripheral blood cleave lipoprotein(a) and apolipoprotein(a) at multiple interkringle sites via the enzyme elastase. Generation of mini-Lp(a) particles and apo(a) fragments. *J. Biol. Chem.* **272**, 11079–11087 (1997).
76. Grenard, J. L. *et al.* Depression and medication adherence in the treatment of chronic diseases in the United States: A meta-analysis. *J. Gen. Intern. Med.* **26**, 1175–1182 (2011).
77. Gehi, A., Haas, D., Pipkin, S. & Whooley, M. A. Depression and medication adherence in outpatients with coronary heart disease: Findings from the heart and soul study. *Arch. Intern. Med.* **165**, 2508–2513 (2005).
78. Goldstein, C. M., Gathright, E. C. & Garcia, S. Relationship between depression and medication adherence in cardiovascular disease: the perfect challenge for the integrated care team. *Patient Prefer. Adherence* **Volume 11**, 547–559 (2017).
79. Morgan, B. M. *et al.* Nonsynonymous SNPs in LPA homologous to plasminogen deficiency mutants represent novel null apo(a) alleles. *J. Lipid Res.* **61**, 432–444 (2020).
80. Schindelin, J. *et al.* Fiji: an open-source platform for biological-image analysis. *Nat. Methods* **9**, 676–82 (2012).

**Figure legends**

**Figure 1: Lp(a) uptake in liver cells is regulated by macropinocytosis. (A)** Representative images of HepG2 cells incubated with Lp(a) for 1 hour following $H_2O$ vehicle (left panel) or 2.5 mM EGTA (right panel) treatment for 1 hour. **(B)** Percentage of Lp(a) vesicles detected in EGTA treated cells compared to vehicle control. **(C)** Representative images of HepG2 cells incubated with Lp(a) for 1 hour following DMSO vehicle (left panel) or 50µM EIPA (right panel) treatment for 1 hour. **(D)** Percentage of Lp(a) vesicles detected in EIPA treated cells compared to vehicle control. **(E)** Representative images of HepG2 cells incubated with apo(a)-mScarlet for 1 hour following DMSO vehicle (left panel) or 50µM EIPA (right panel) treatment for 1 hour. **(F)** Percentage of apo(a)-mScarlet vesicles detected in EIPA treated cells compared to vehicle control. *= p<0.05, **= p<0.01 from one sample T-test comparing values to vehicle treated controls normalised to 100%. Data points represent means of independent experiments quantified from 5 fields of view of ~20 cells per field from each independent experiment. Error bars represent standard error of the mean. Lp(a) was detected using the LPA4 primary antibody and AlexaFluor conjugated anti-mouse secondary antibody. Apo(a)-mScarlet was directly detected. Images were acquired on an Olympus FV1000/FV1200 confocal microscope. Scale bar= 5 µM.

**Figure 2: Lp(a) macropinocytosis is inhibited by antidepressants in macrophages. (A)** Representative images of PMA-differentiated THP-1 cells incubated with Lp(a) for 1 hour following $H_2O$ vehicle (left panel) or 2.5 mM EGTA (right panel) treatment for 1 hour. **(B)** Percentage of Lp(a) vesicles detected in EGTA treated cells compared to vehicle control. **(C)** Representative images of PMA-differentiated THP-1 cells incubated with Lp(a) for 1 hour following DMSO vehicle (left panel) or 1 mM amiloride (right panel) treatment for 1 hour. **(D)** Percentage of Lp(a) vesicles detected in amiloride treated cells compared to vehicle control. **(E)** Representative images of PMA-differentiated THP-1 cells incubated with Lp(a) for 1 hour following $H_2O$ vehicle, 20 µM imipramine, 50 µM citalopram, 20 µM fluoxetine or 20 µM sertraline (left to right) treatment overnight. **(F)** Representative images of PMA-differentiated THP-1 cells incubated 70 kDa dextran-TRITC for 1 hour following $H_2O$ vehicle or 20 µM imipramine, 50 µM citalopram, 20 µM fluoxetine or 20 µM sertraline (left to right) treatment overnight. **(G)** Percentage of Lp(a) vesicles detected in antidepressant treated cells compared to vehicle control. **(H)** Percentage of dextran-TRITC vesicles detected in antidepressant treated cells compared to vehicle control. n.s= not significant, *= p<0.05, **=p<0.01 from a one sample t-test **(B)**, **(D)** or randomised block ANOVA **(G)**, **(H)** comparing treated cells to vehicle control. Data points represent means of independent experiments quantified from 5 fields of view of ~20 cells per field from each independent experiment. Error bars represent standard error of the mean. Lp(a) was detected using the LPA4 primary antibody and AlexaFluor conjugated anti-mouse secondary antibody. 70 kDa dextran-TRITC was detected directly. Images were acquired on an Olympus FV1000/FV3000 confocal microscope. Scale bar= 5 µM.

**Figure 3: Antidepressants have variable effects on Lp(a) uptake in liver cells. (A)** Representative images of HepG2 cells incubated with Lp(a) for 1 hour following $H_2O$ vehicle (left) or 20 µM imipramine (right panel) treatment overnight. **(B)** Percentage of Lp(a) vesicles detected following overnight treatment with 5, 10, and 20 µM imipramine compared to vehicle control. **(C)** Percentage of Lp(a) vesicles detected in 20 µM imipramine treated cells compared to vehicle control. **(D)** Representative images of HepG2 cells incubated with Lp(a) for 1 hour following $H_2O$ vehicle (left) or 50 µM citalopram (right panel) treatment overnight. **(E)** Percentage of Lp(a) vesicles detected following overnight treatment with 5, 10, 20 and 50 µM citalopram compared to vehicle control. **(F)** Percentage of Lp(a) vesicles detected in 50 µM citalopram treated cells compared to vehicle control. **(G)** Representative images of HepG2 cells incubated with Lp(a) for 1 hour following $H_2O$ vehicle (left) or 20 µM fluoxetine (right) for 2 hours. **(H)** Percentage of Lp(a) vesicles detected following 2 hours treatment with 5, 10, and 20 µM fluoxetine compared to vehicle control. **(I)** Percentage of Lp(a) vesicles detected in 20 µM fluoxetine treated cells compared to vehicle control. **(J)** Representative images of HepG2 cells incubated with Lp(a) for 1 hour following $H_2O$ vehicle (left) or 20 µM sertraline (right) for 2 hours. **(K)** Percentage of Lp(a) vesicles detected following 2 hours treatment with 5, 10, and 20 µM sertraline compared to vehicle control. **(L)** Percentage of Lp(a) vesicles detected in 20 µM sertraline treated cells compared to vehicle control. **(M)** Representative images of HepG2 cells incubated with 70kDa dextran-TRITC for 1 hour following $H_2O$ vehicle (left to right), 20 µM imipramine (overnight), 50 µM citalopram (overnight), 20 µM fluoxetine (2 hours) and 20 µM sertraline (2 hours) treatment. **(N)** Percentage of 70 kDa dextran-TRITC vesicles detected following treatment with antidepressants compared to vehicle control. n.s. = not significant, *= p<0.05, **=p<0.01 from one sample T-test comparing values to vehicle treated controls normalised to 100% **(I)**, **(L)**, Wilcoxon rank sum test **(C, F)** or randomised-block ANOVA **(N)**. Data points represent means of independent experiments quantified from 5 fields of view of ~20 cells per field from each independent experiment. Error bars represent standard error of the mean. Lp(a) was detected using the LPA4 primary antibody and AlexaFluor conjugated anti-mouse secondary antibody. Images were acquired on an Olympus FV1000/FV1200 confocal microscope. Scale bar= 5 µM.

**Figure 4: Antidepressants specifically increase Lp(a) surface binding in liver cells. (A)** Representative images of maximum z-projections of surface-bound Lp(a) following $H_2O$ vehicle, 20 µM imipramine or 50 µM citalopram treatment overnight. **(B)** Surface Lp(a) signal per cell in vehicle, imipramine and citalopram treated cells. **(C)** Representative images of maximum z-projections of surface-bound dextran following $H_2O$ vehicle, 20 µM imipramine or 50 µM citalopram treatment overnight. **(D)** Surface dextran signal per cell in vehicle, imipramine and citalopram treated cells. **(E)** Representative SEM images of HepG2 cells incubated with $H_2O$ vehicle or 50 µM citalopram overnight. **(F)** Quantification of membrane ruffling events per cell in vehicle and citalopram treated cells. n.s. = not significant, *= p<0.05, p=<0.01 from randomised block ANOVA comparing treated to vehicle control conditions **(B,D,F)**. Data points represent means of independent experiments quantified from 5 fields of view of ~20 cells per field from each independent experiment **(B,D,F)**. Data points represent single cells **(H)**. Error bars represent standard error of the mean. 70 kDa dextran-TRITC was detected directly. Lp(a) was detected using the LPA4 primary antibody and AlexaFluor conjugated anti-mouse secondary antibody. Images were acquired on an Olympus FV1000/FV1200 confocal microscope **(A,C,E)** or an FEI Nova NanoSEM **(G).** Scale bar= 5 µM **(A,C,E)** or 2 µM **(G)**.

**Figure 5: Serotonin increases Lp(a) surface binding and macropinocytosis. (A)** Representative images of maximum z-projections of surface-bound Lp(a) following $H_2O$ vehicle (left) or 0.5 mM serotonin treatment (right) overnight. **(B)** Surface Lp(a) signal per cell in vehicle or serotonin treated cells. **(C)** Representative images of endocytosed Lp(a) following $H_2O$ and DMSO vehicle (left), 0.5 mM serotonin (middle) or 0.5 mM serotonin and 50 µM EIPA overnight (1 hour for EIPA) and incubation with Lp(a) for 1 hour. **(D)** Lp(a) vesicles per cell in vehicle, serotonin or serotonin + EIPA treated cells. **(E)** Percentage change in Lp(a) vesicle number compared to vehicle with serotonin or serotonin + EIPA treatment. **(F)** Representative images of maximum z-projections of surface-bound dextran following $H_2O$ vehicle (left) or 0.5 mM serotonin treatment (right) overnight. **(G)** Surface dextran signal per cell in vehicle or serotonin treated cells. **(H)** Representative images of endocytosed dextran following $H_2O$

and DMSO vehicle (left), 0.5 mM serotonin (middle) or 0.5 mM serotonin and 50 µM EIPA overnight (1 hour for EIPA) and incubation with dextran for 1 hour. **(I)** Percentage change in dextran vesicle number compared to vehicle with serotonin treatment. n.s. = not significant, *= p<0.05, **p=<0.01 from unpaired Student's T-test **(B,G)** randomised block ANOVA comparing treated to vehicle control **(D)** or one-sample T-test **(E,I)**. Data points represent means of independent experiments quantified from 5 fields of view of ~20 cells per field from each independent experiment. Error bars represent standard error of the mean. 70 kDa dextran-TRITC was detected directly. Lp(a) was detected using the LPA4 primary antibody and AlexaFluor$^{488}$ secondary antibody. Images were acquired on an Olympus FV1000 confocal microscope**.** Scale bar= 5 µM.

**Figure 6: Imipramine and citalopram enhance Lp(a) delivery to Rab11$^{+}$ recycling endosomes. (A)** Representative images of HepG2 cells incubated with Lp(a) for 30 minutes following $H_2O$ vehicle (top panel), 20 µM imipramine (middle panel) or 50 µM citalopram (bottom panel) overnight. Cells were co-stained with anti-LPA4 (magenta) and anti-Rab11 (green) and detected with AlexaFluor secondary antibodies. **(B)** Representative images of HepG2 cells incubated with Lp(a) for 120 minutes following $H_2O$ vehicle (top panel), 20 µM imipramine (middle panel) or 50 µM citalopram (bottom panel) overnight. Cells were co-stained with anti-LPA4 (magenta) and anti-Rab11 (green). **(C)** Representative images of HepG2 cells incubated with Lp(a) for 30 minutes following $H_2O$ vehicle (top panel), 20 µM imipramine (middle panel) or 50 µM citalopram (bottom panel) overnight. Cells were co-stained with anti-LPA4 (magenta) and anti-Rab7 (green) and detected with AlexaFluor secondary antibodies. **(D)** Representative images of HepG2 cells incubated with Lp(a) for 120 minutes following $H_2O$ vehicle (top panel), 20 µM imipramine (middle panel) or 50 µM citalopram (bottom panel) overnight. Cells were co-stained with anti-LPA4 (magenta) and anti-Rab7 (green). **(E)** Quantification of percentage vesicle overlap between Lp(a) and Rab11 channels. **(F)** Quantification of percentage vesicle overlap between Lp(a) and Rab7 channels. n.s.= not significant, *= p<0.05, **= p<0.01 from randomised block ANOVA comparing treated to vehicle control conditions at each timepoint. Data points represent means of independent experiments quantified from 5 fields of view of ~20 cells per field from each independent experiment. Error bars represent standard error of the mean. Images were acquired on an Olympus FV1000/FV1200 confocal microscope. Scale bar= 5 µM.

**Figure 7: Imipramine and citalopram stimulate Lp(a) and apo(a) recycling. (A)** Representative Western blots of HepG2 cells treated with vehicle ($H_2O$), 20 µM imipramine or 50 µM citalopram and incubated with Lp(a) for 2 hours, after which Lp(a) containing media was removed and replaced with fresh Lp(a)-free media and lysates collected immediately or after 2 or 6 hours (labelled 0, 2 and 6 hr, respectively). **(B)** Quantification of Lp(a) band intensity normalised to actin band intensity at 0, 2 and 6 hours with vehicle, imipramine or citalopram treatment. **(C)** Representative Western blots of Lp(a) immunoprecipitated from fresh cell media collected 0, 2 or 6 hours after vehicle, imipramine or citalopram treated HepG2 were incubated with Lp(a) for 2 hours in **(A)**. **(D)** Quantification of total immunoprecipitated Lp(a) band intensity 2- and 6-hours following removal of Lp(a) containing media. **(E)** Representative Western blots of HepG2 cells treated with vehicle ($H_2O$), 20 µM imipramine or 50 µM citalopram and incubated with apo(a)-mScarlet/tGFP for 2 hours, after which apo(a)-mScarlet/tGFP containing media was removed and replaced with fresh apo(a)-mScarlet/tGFP-free media and lysates collected immediately or after 2 or 6 hours (labelled 0, 2 and 6 hr, respectively). **(F)** Quantification of apo(a)-mScarlet/tGFP band intensity normalised to actin band intensity at 0, 2 and 6 hours with vehicle, imipramine or citalopram treatment. **(G)** Representative Western blots of apo(a)-mScarlet/tGFP immunoprecipitated from fresh cell media collected 0, 2 or 6 hours after vehicle, imipramine or citalopram treated HepG2 were incubated with apo(a)-mScarlet/tGFP for 2 hours in **(E)**. **(H)** Quantification of total immunoprecipitated apo(a)-mScarlet/tGFP band intensity 2- and 6-hours following removal of apo(a)-mScarlet/tGFP containing media. n.s.= not significant, *= p<0.05, **= p<0.01 from randomised block ANOVA. Data points represent means of independent experiments. Error bars represent standard error of the mean.

**Figure 8: Summary of the effects of antidepressants on Lp(a) uptake and subcellular trafficking in liver cells.** Imipramine and citalopram enhance Lp(a) binding to the cell surface, resulting in increased Lp(a) engulfment by macropinocytosis. Sertraline inhibits Lp(a) uptake via macropinocytosis into the cell. Imipramine and citalopram increase the sorting of Lp(a) into Rab11-positive recycling endosomes, but not Rab7 or LAMP1 positive compartments. As a consequence of increased delivery into Rab11-postive recycling endosomes, imipramine and citalopram lead to increased recycling of apo(a) back into the cellular media.

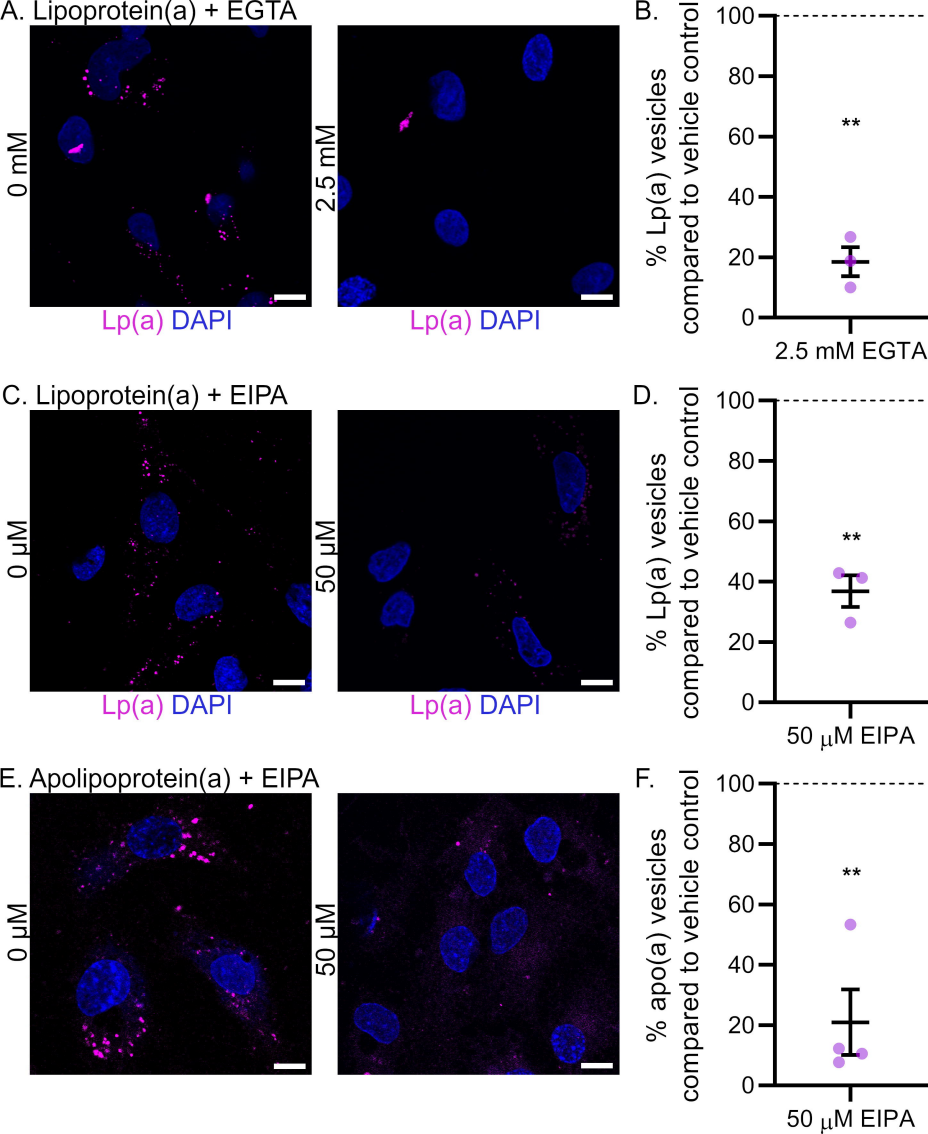
A. Lipoprotein(a) + EGTA
0 mM
2.5 mM
Lp(a) DAPI
Lp(a) DAPI
B.
% Lp(a) vesicles compared to vehicle control
100
80
60
40
20
0
**
2.5 mM EGTA
C. Lipoprotein(a) + EIPA
0 µM
50 µM
Lp(a) DAPI
Lp(a) DAPI
D.
% Lp(a) vesicles compared to vehicle control
100
80
60
40
20
0
**
50 µM EIPA
E. Apolipoprotein(a) + EIPA
0 µM
50 µM
F.
% apo(a) vesicles compared to vehicle control
100
80
60
40
20
0
**
50 µM EIPA

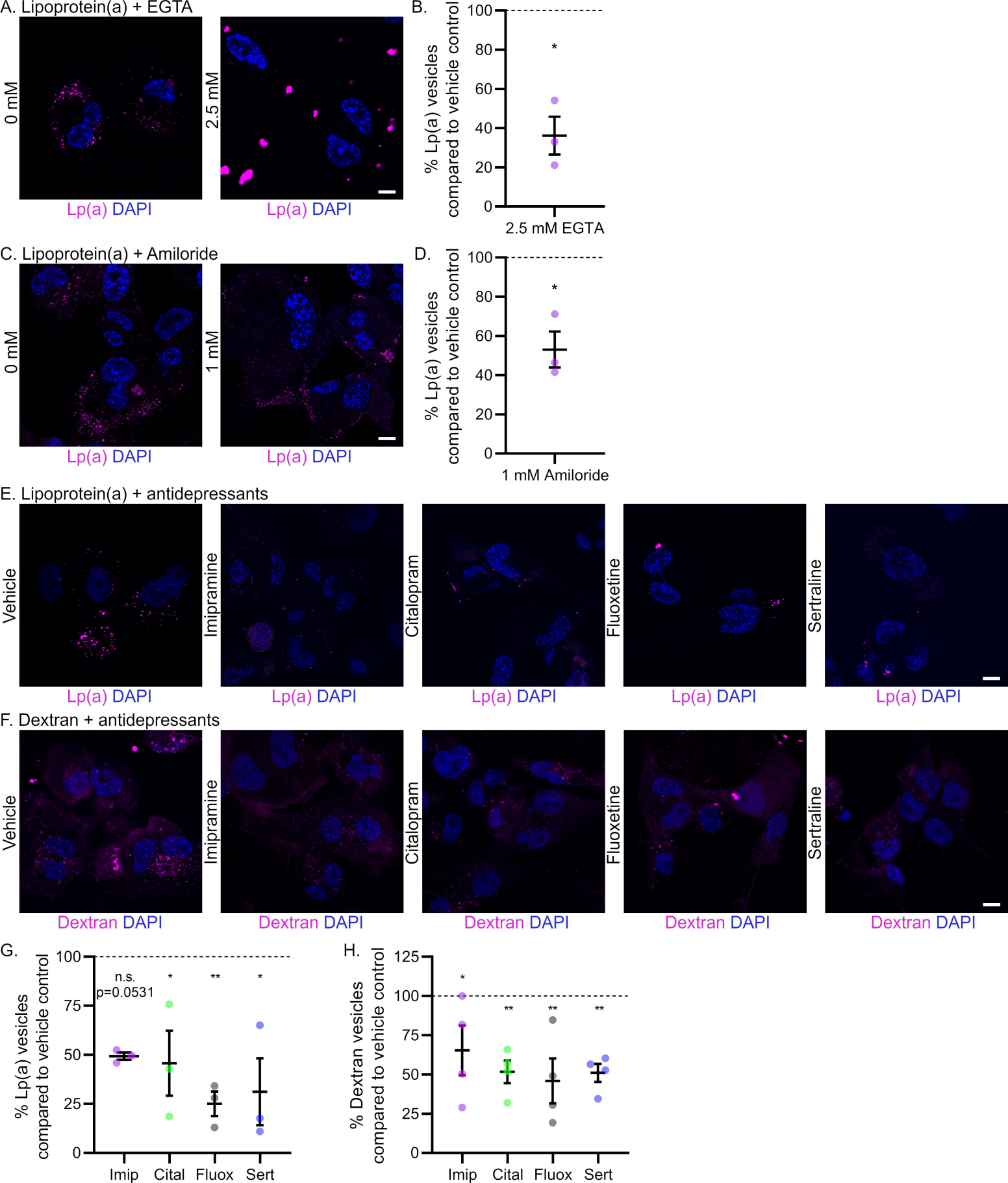
A. Lipoprotein(a) + EGTA
0 mM
2.5 mM
Lp(a) DAPI
Lp(a) DAPI
B.
% Lp(a) vesicles compared to vehicle control
100
80
60
40
20
0
*
2.5 mM EGTA
C. Lipoprotein(a) + Amiloride
0 mM
1 mM
Lp(a) DAPI
Lp(a) DAPI
D.
% Lp(a) vesicles compared to vehicle control
100
80
60
40
20
0
*
1 mM Amiloride
E. Lipoprotein(a) + antidepressants
Vehicle
Imipramine
Citalopram
Fluoxetine
Sertraline
Lp(a) DAPI
Lp(a) DAPI
Lp(a) DAPI
Lp(a) DAPI
Lp(a) DAPI
F. Dextran + antidepressants
Vehicle
Imipramine
Citalopram
Fluoxetine
Sertraline
Dextran DAPI
Dextran DAPI
Dextran DAPI
Dextran DAPI
Dextran DAPI
G.
% Lp(a) vesicles compared to vehicle control
100
75
50
25
0
n.s.
p=0.0531
*
**
*
Imip
Cital
Fluox
Sert
H.
% Dextran vesicles compared to vehicle control
125
100
75
50
25
0
*
**
**
**
Imip
Cital
Fluox
Sert

A. Lipoprotein(a) + Imipramine

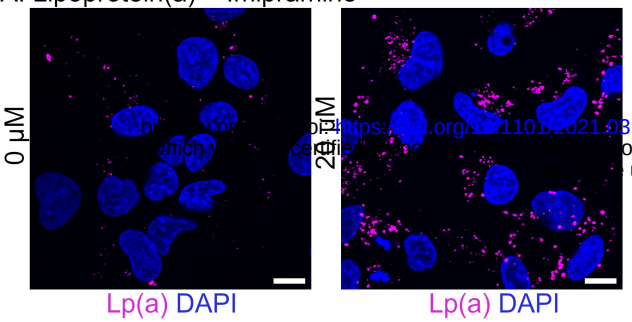


B.

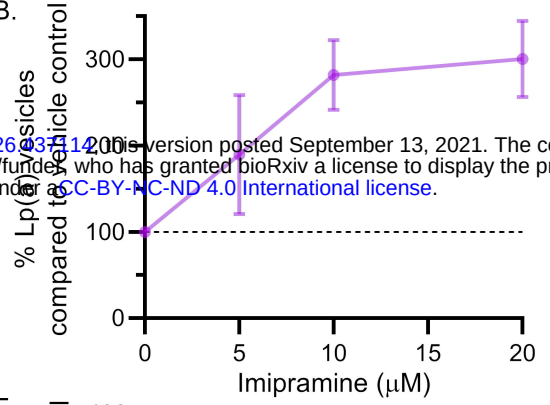


C.

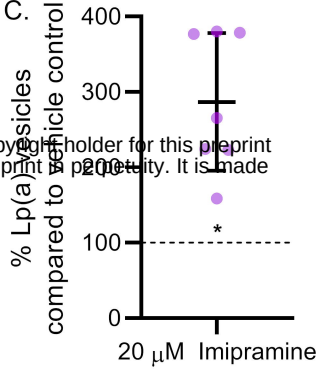


D. Lipoprotein(a) + Citalopram

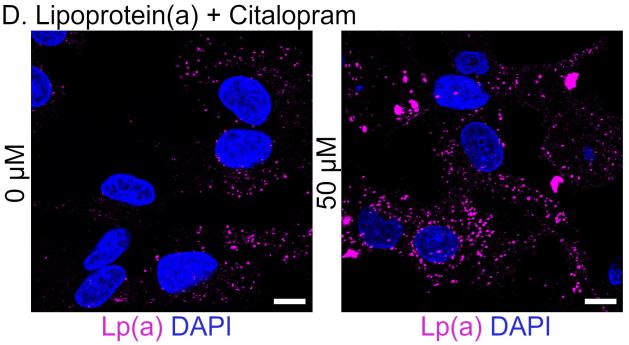


E.

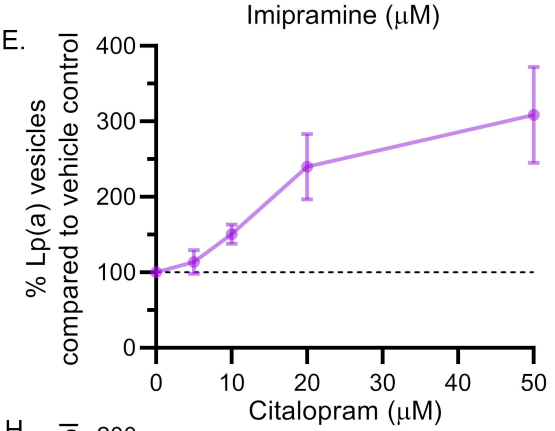


F.

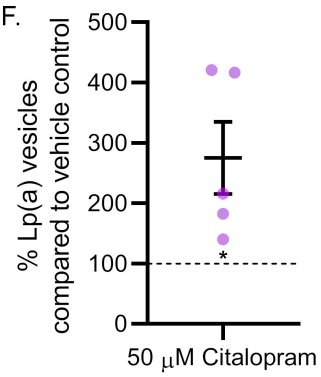


G. Lipoprotein(a) + Fluoxetine

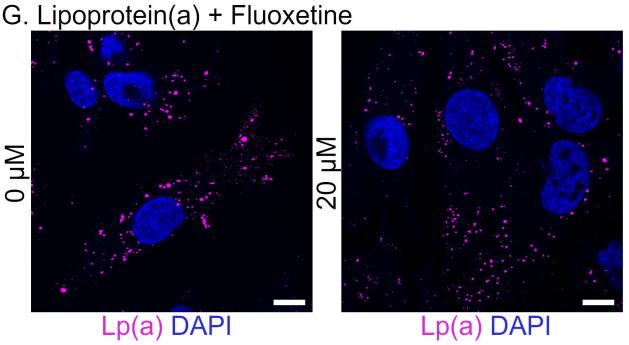


H.

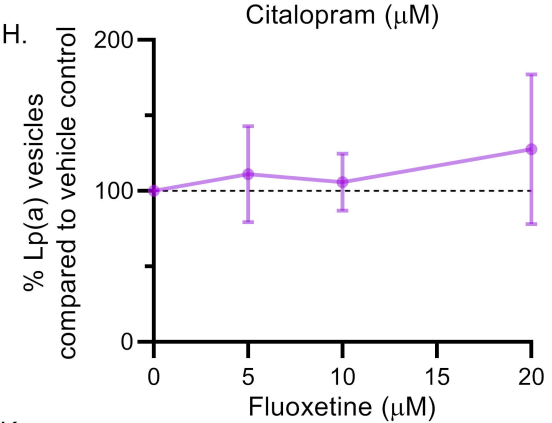


I.

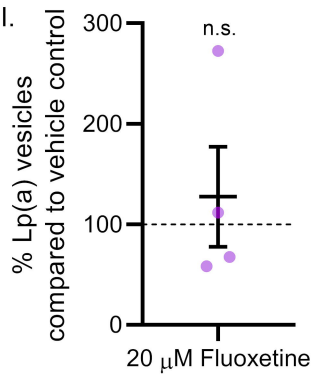


J. Lipoprotein(a) + Sertraline

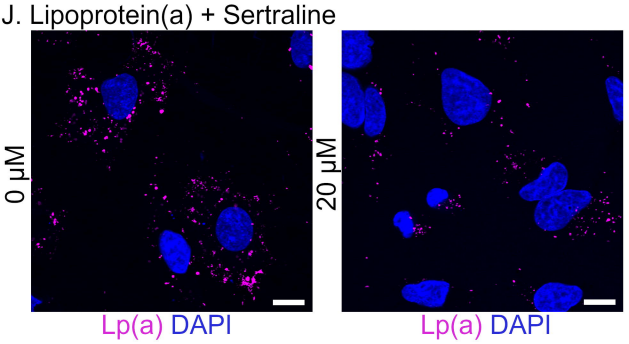


K.

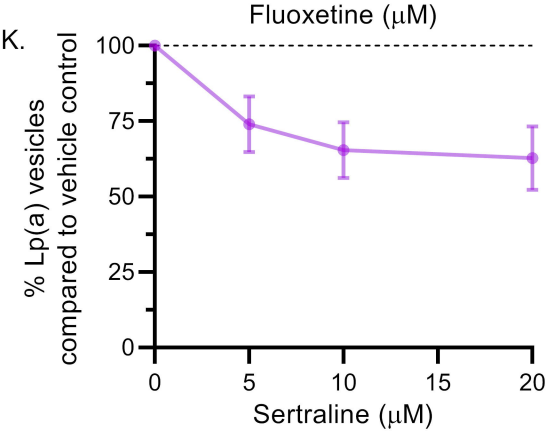


L.

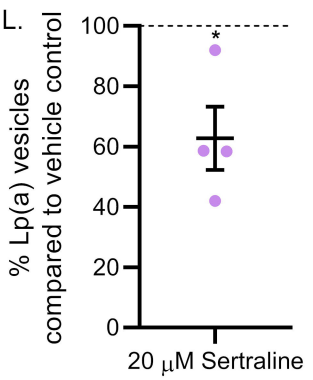


M. Dextran + antidepressants

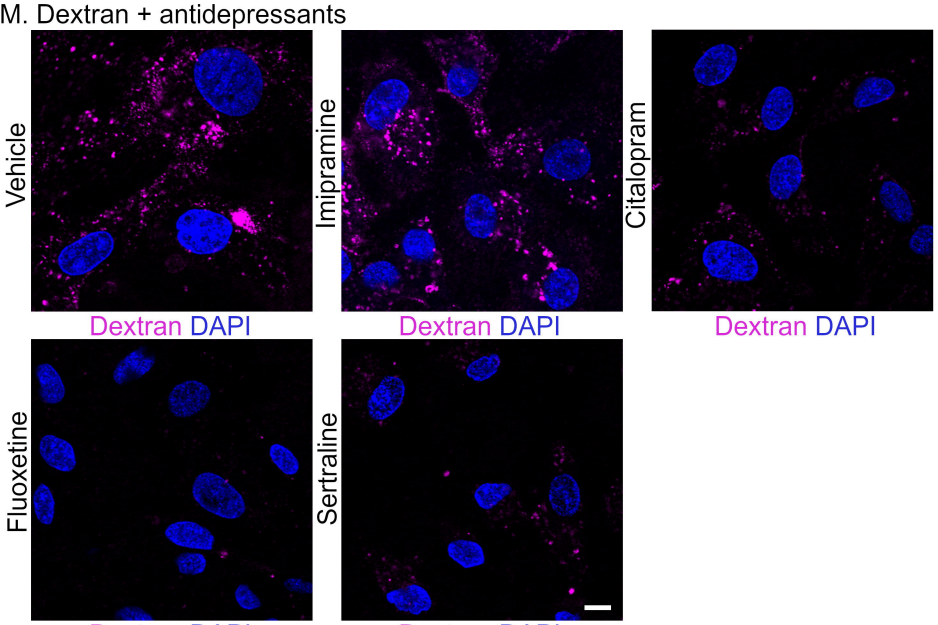


N.

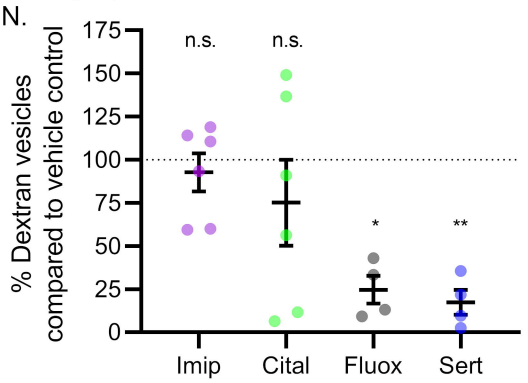

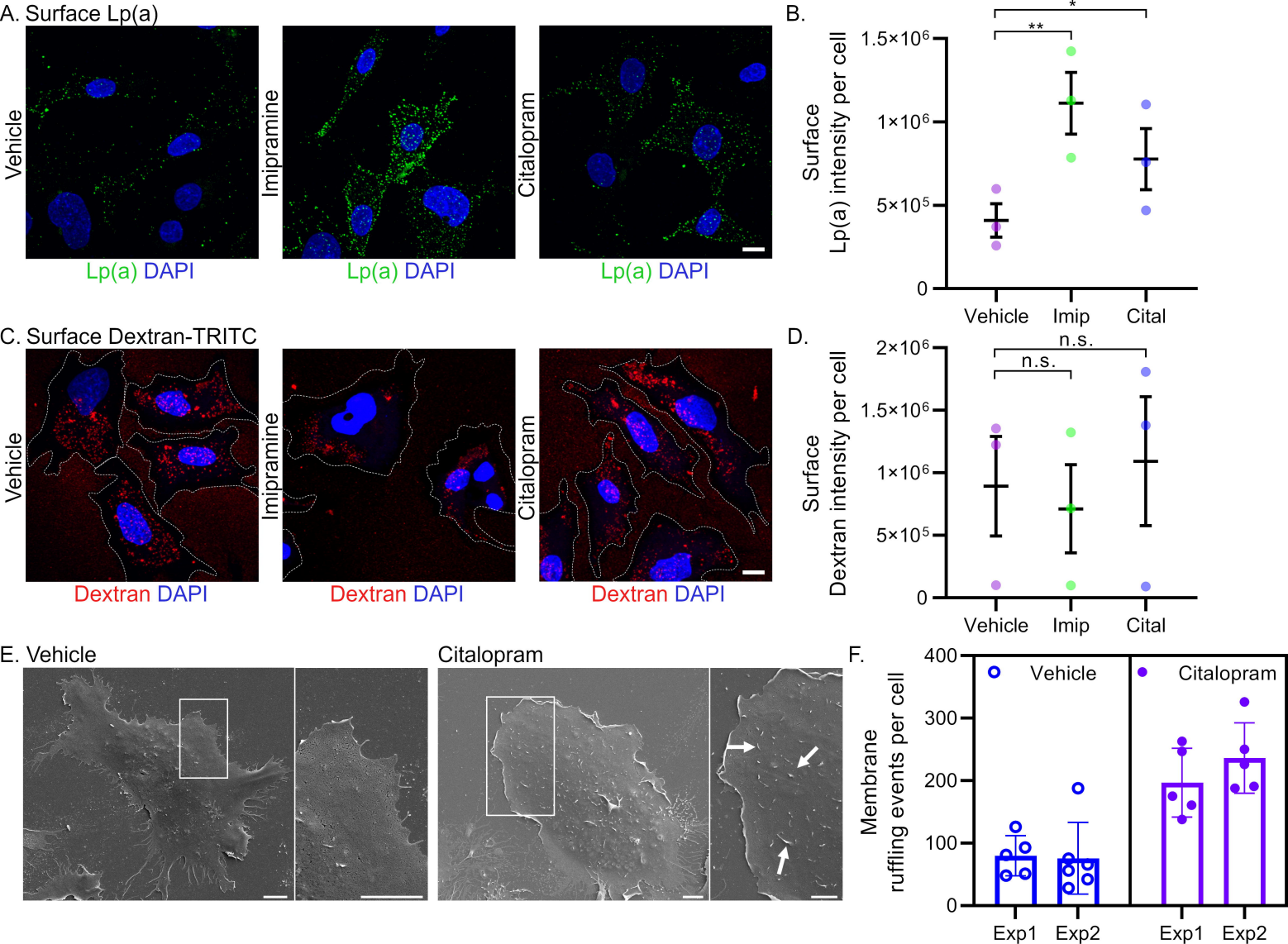
A. Surface Lp(a)
Vehicle
Imipramine
Citalopram
Lp(a) DAPI
Lp(a) DAPI
Lp(a) DAPI
B.
Surface Lp(a) intensity per cell
1.5×10^6
1×10^6
5×10^5
0
*
**
Vehicle
Imip
Cital
C. Surface Dextran-TRITC
Vehicle
Imipramine
Citalopram
Dextran DAPI
Dextran DAPI
Dextran DAPI
D.
Surface Dextran intensity per cell
2×10^6
1.5×10^6
1×10^6
5×10^5
0
n.s.
n.s.
Vehicle
Imip
Cital
E. Vehicle
Citalopram
F.
Membrane ruffling events per cell
400
300
200
100
0
Vehicle
Citalopram
Exp1
Exp2
Exp1
Exp2

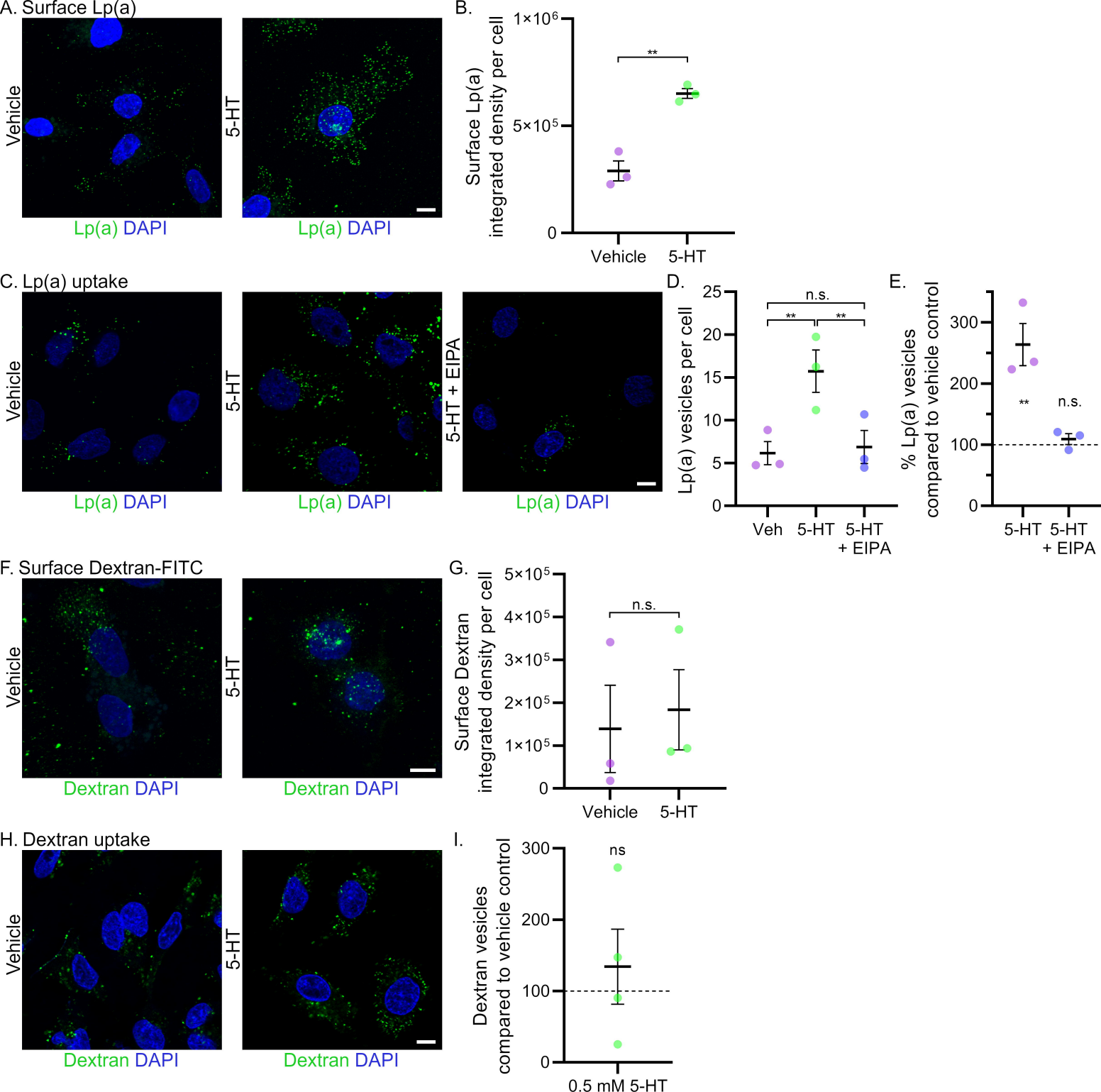
A. Surface Lp(a)
Vehicle
5-HT
Lp(a) DAPI
Lp(a) DAPI
B.
Surface Lp(a) integrated density per cell
1×10^6
5×10^5
0
**
Vehicle
5-HT
C. Lp(a) uptake
Vehicle
5-HT
5-HT + EIPA
Lp(a) DAPI
Lp(a) DAPI
Lp(a) DAPI
D.
Lp(a) vesicles per cell
25
20
15
10
5
0
n.s.
**
**
Veh
5-HT
5-HT + EIPA
E.
% Lp(a) vesicles compared to vehicle control
300
200
100
0
**
n.s.
5-HT
5-HT + EIPA
F. Surface Dextran-FITC
Vehicle
5-HT
Dextran DAPI
Dextran DAPI
G.
Surface Dextran integrated density per cell
5×10^5
4×10^5
3×10^5
2×10^5
1×10^5
0
n.s.
Vehicle
5-HT
H. Dextran uptake
Vehicle
5-HT
Dextran DAPI
Dextran DAPI
I.
Dextran vesicles compared to vehicle control
300
200
100
0
ns
0.5 mM 5-HT

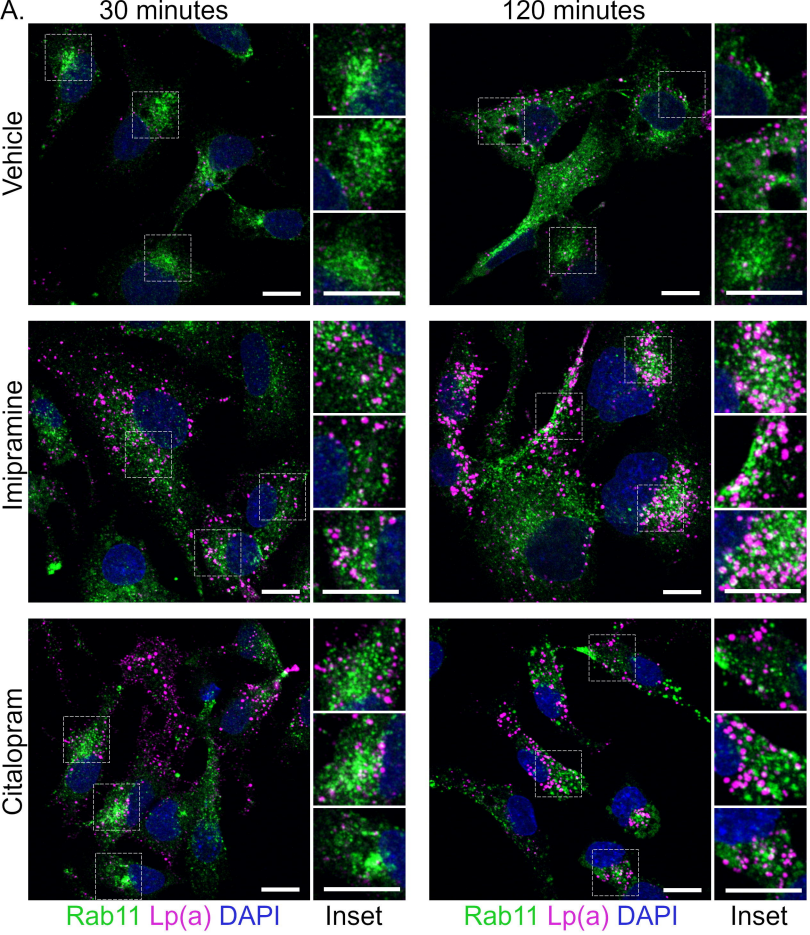
A.
30 minutes
120 minutes
Vehicle
Imipramine
Citalopram
Rab11 Lp(a) DAPI
Inset
Rab11 Lp(a) DAPI
Inset

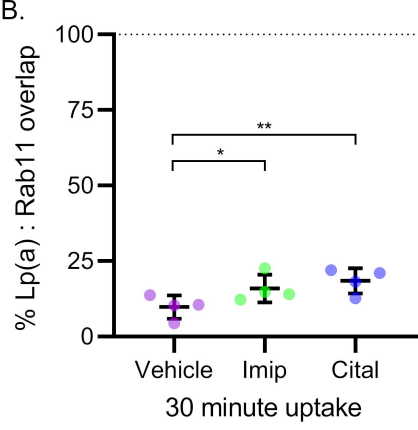
B.
% Lp(a) : Rab11 overlap
100
75
50
25
0
**
*
Vehicle
Imip
Cital
30 minute uptake

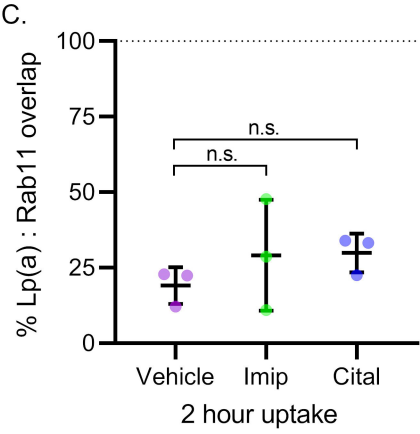
C.
% Lp(a) : Rab11 overlap
100
75
50
25
0
n.s.
n.s.
Vehicle
Imip
Cital
2 hour uptake

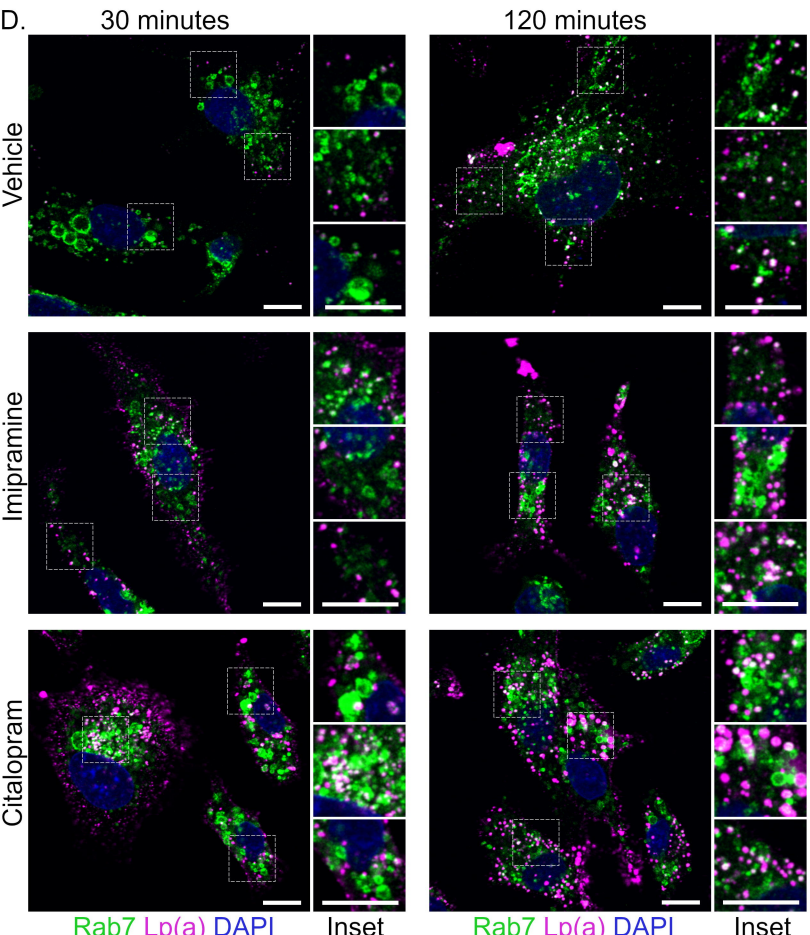
D.
30 minutes
120 minutes
Vehicle
Imipramine
Citalopram
Rab7 Lp(a) DAPI
Inset
Rab7 Lp(a) DAPI
Inset

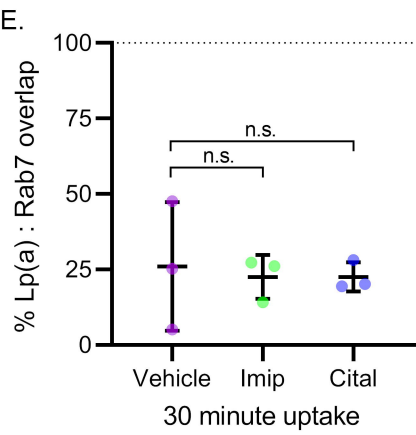
E.
% Lp(a) : Rab7 overlap
100
75
50
25
0
n.s.
n.s.
Vehicle
Imip
Cital
30 minute uptake

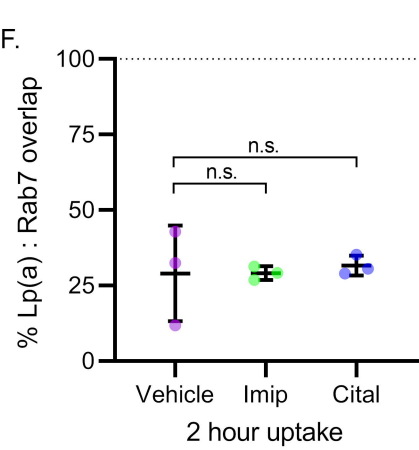
F.
% Lp(a) : Rab7 overlap
100
75
50
25
0
n.s.
n.s.
Vehicle
Imip
Cital
2 hour uptake

A. Internalised Lp(a)

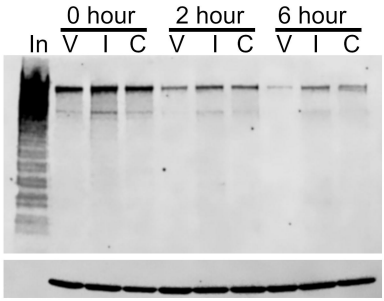


B.

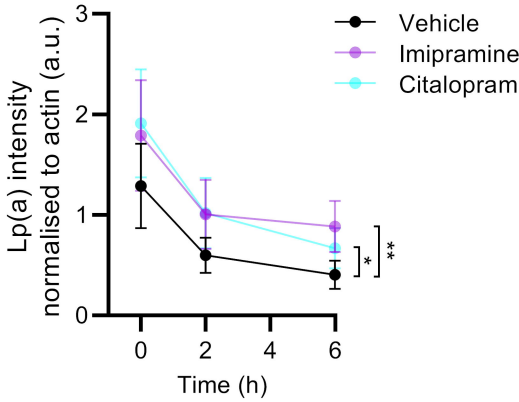


C. Recycled Lp(a)

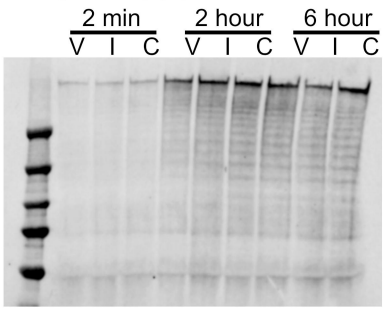


D.

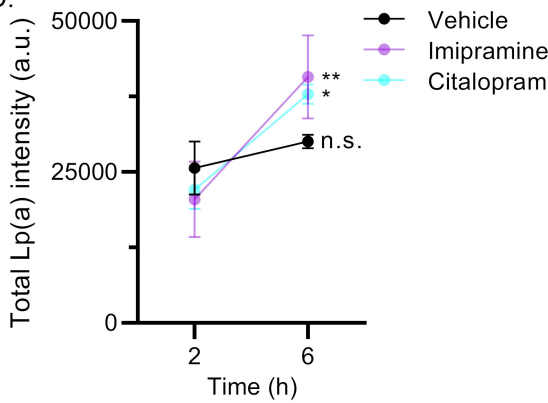


E. Internalised apo(a)

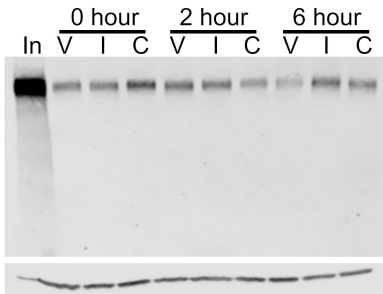


F.

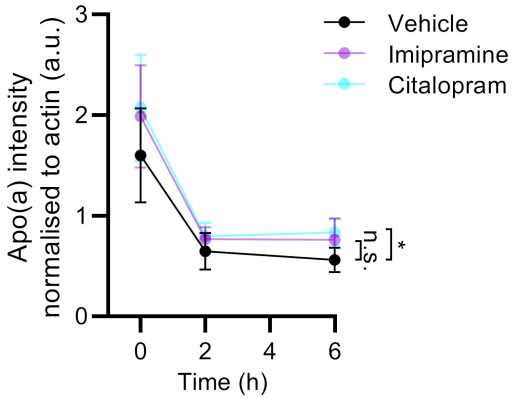


G. Recycled apo(a)

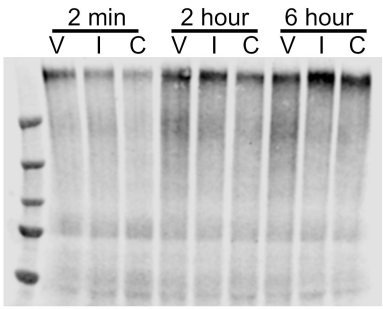


H.

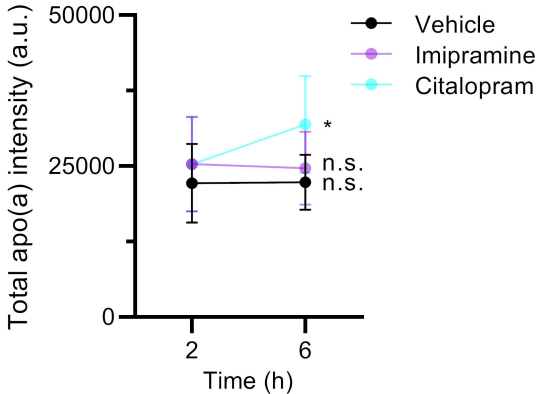

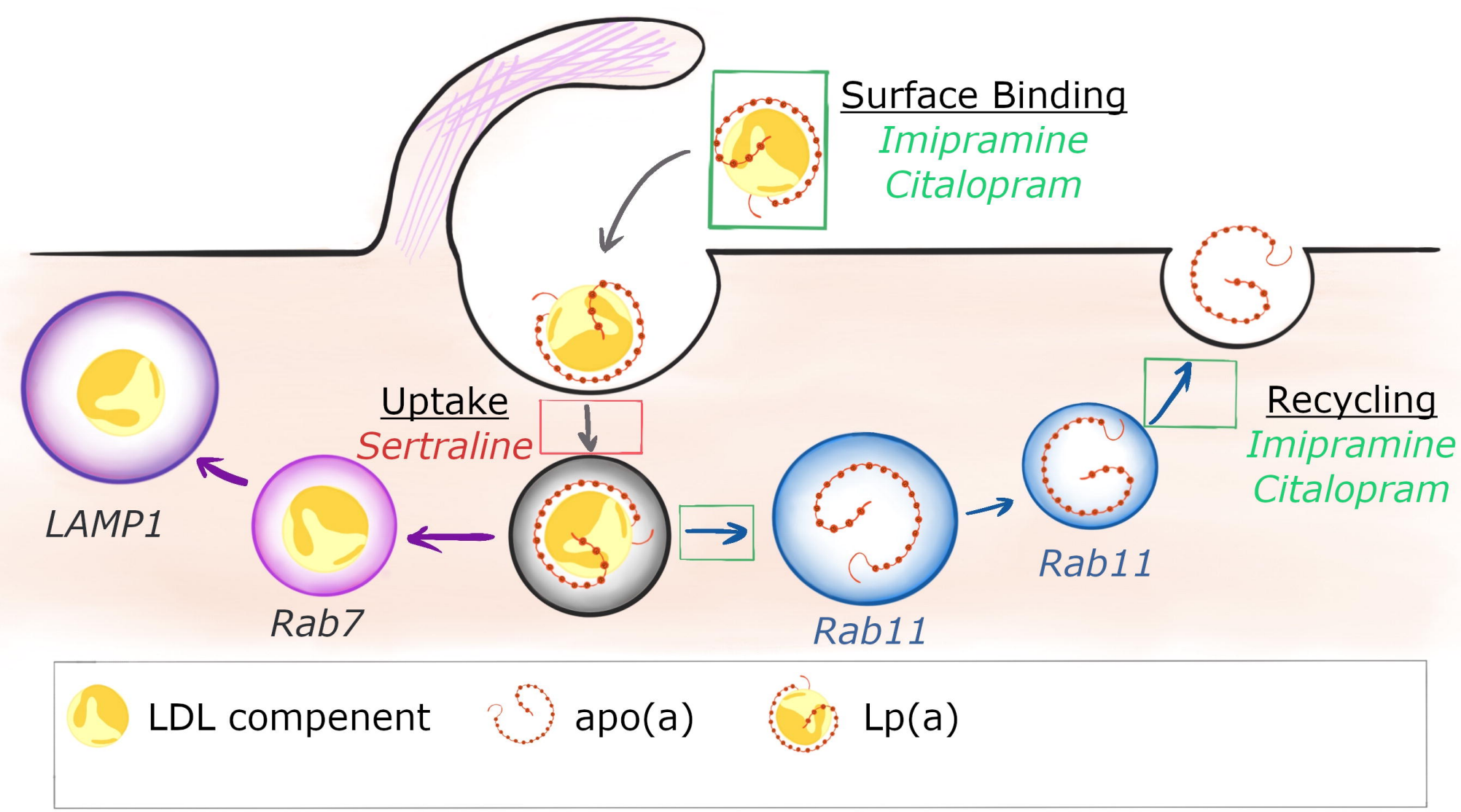
Surface Binding
Imipramine
Citalopram
Uptake
Sertraline
Recycling
Imipramine
Citalopram
LAMP1
Rab7
Rab11
Rab11
LDL compenent
apo(a)
Lp(a)